Novel styryl-indoles as small molecule inhibitors of 25-hydroxyvitamin D-24-hydroxylase (CYP24A1): Synthesis and biological evaluation

Salvatore Ferla,[a] Mohamed S. Gomaa,[a†] Andrea Brancale,[a] Jinge Zhu,[b] Justin T. Ochalek,[b] Hector F. DeLuca[b] and Claire Simons[a*]

[a]*Medicinal Chemistry, School of Pharmacy & Pharmaceutical Sciences, Cardiff University, King Edward VII Avenue, Cardiff CF10 3NB, UK;* [b]*Department of Biochemistry, University of Wisconsin-Madison, 433 Babcock Drive, Madison, WI 53706-1544, USA.*

* Corresponding author. Tel: +44-(0)-2920-876307; fax: +44-(0)2920-874149.

E-mail address: SimonsC@Cardiff.ac.uk (Claire Simons)

URL: http://www.cardiff.ac.uk/phrmy/staffinfo/CS/homepage/CS.html

[†]Present address: Pharmaceutical Chemistry Department, Faculty of Pharmacy, Suez Canal University, Egypt

Abstract

The synthesis of a series of imidazole styrylindoles and sulfonyl styrylindoles derivatives is described. Evaluation of binding affinity and inhibitory activity against CYP24A1 identified the imidazole styrylindoles as potent inhibitors with activity greater or comparable with the standard ketoconazole.

Flexible alignment and docking studies of the inhibitors in the CYP24A1 enzyme active site confirmed that complete occupation of the vitamin D access tunnel is essential to inhibitory activity, allowing exposure to multiple hydrophobic binding interactions and optimal conformation for the interaction of the imidazole nitrogen lone pair and the active site haem.

Highlights

- New series of imidazole styrylindoles and sulfonyl styrylindoles synthesized.
- Compounds evaluated as inhibitors of 25-hydroxyvitamin D-24-hydroxylase (CYP24A1).
- Imidazole series potent CYP24A1 inhibitors.
- Computational studies identified key enzyme binding interactions.

Key words: imidazole styrylindoles; sulfonyl styrylindoles; CYP24A1; vitamin D; molecular modeling

1. Introduction

The most biologically active form of vitamin D_3, 1α,25-dihydroxyvitamin D_3 ($1,25(OH)_2D_3$, calcitriol, **1**) has an important role in the regulation of cell proliferation and differentiation [1] in addition to the key role of calcitriol in the regulation of calcium homeostasis and bone metabolism [2], [3]. Serum levels of calcitriol have been associated with the prognosis of several cancers, with higher serum levels associated with improved prognosis [4], [5], [6] and lower levels associated with an increased risk and poorer prognosis [7], [8], [9], [10]. The serum level of calcitriol is tightly regulated in a short feedback loop by two cytochrome P450 enzymes, the 1α-hydroxylase CYP27B1 that promotes synthesis of calcitriol and the 24-hydroxylase CYP24A1 that inactivates calcitriol by metabolism [11], [12]. Lower calcitriol levels is directly linked to high expression of *CYP24A1* with increased CYP24A1 levels resulting in increased metabolism of calcitriol significantly reducing the circulating calcitriol and therefore the antiproliferative or prodifferentiation effects [13], [14], [15], [16].

Inhibition of CYP24A1 is therefore an attractive strategy to enhance endogenous circulating calcitriol and/or increase the half-life of exogenously administered calcitriol or vitamin D therapeutic. Studies using the non-specific CYP inhibitors, ketoconazole or liarozole in combination with calcitriol in prostate and breast cancer cell lines resulted in increased half-life of calcitriol and enhanced antiproliferative effect [17], [18]. Similarly studies using CYP24A1 inhibitors, the isoflavone genistein and a novel tetralone derivative, greatly enhanced the apoptotic and differention effect of calcitriol in prostate cancer cell lines [19], [20].

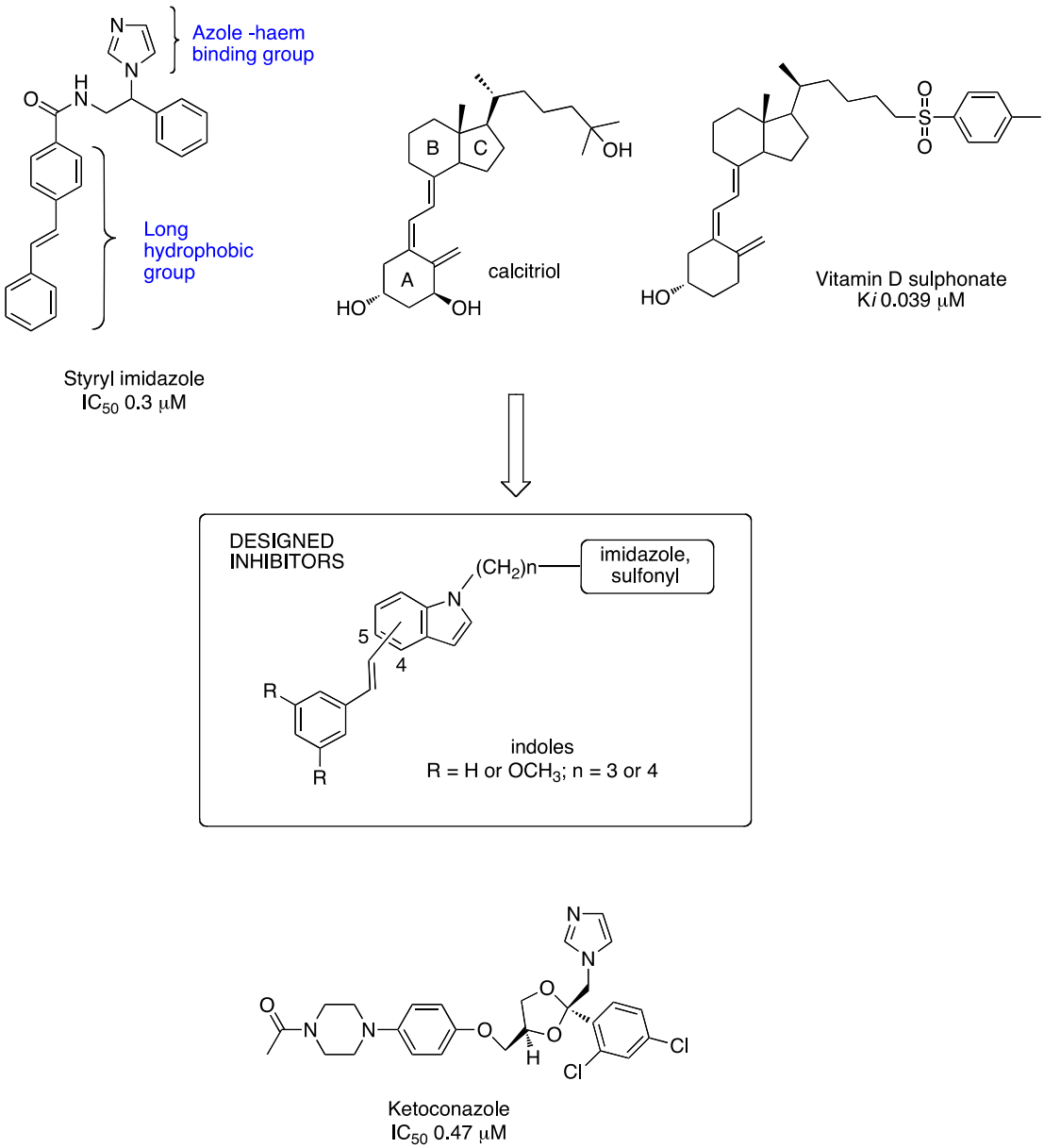

Figure 1. Structures of natural CYP24A1 substrate calcitriol, standard inhibitor for comparison ketoconazole and designed 4- and 5- styrylindole derivatives

Our previous research on non-vitamin D CYP24A1 inhibitors [20], [21], [22] indicated the importance of a hydrophobic group or chain to allow complete fill of the hydrophobic channel of the CYP24A1 enzyme active site. In the development of the azole inhibitors, a styryl group was found to be optimal for inhibitory activity [21] (Figure 1) resulting in compounds with activity comparable with the standard

inhibitor ketoconazole (Figure 1). Combining the styryl and azole haem binding group with an indole group, to mimic the calcitriol C/D ring unit, resulted in the design of the herein described indole imidazole series. In addition a series of indole sulphonyl derivatives was designed based on the very the promising vitamin D sulphonate derivatives [23] (Figure 1).

2. Results

2.1 Chemistry

The styrenes (**3** and **9**) were prepared by Heck reaction of either styrene (**2a**) or 1,3-dimethoxy-5-vinylbenzene (**2b**) with the bromoindole (**1** or **8**) using paladium (II) acetate catalyst, tri(*o*-tolylphosphine) (TOP) as ligand and triethylamine as basic medium at 110 ^{o}C in a sealed tube overnight (Scheme 1) [24]. The indole bromoalkyl derivatives with either a lateral three carbon chain (**4**, **10**) or lateral four carbon chain (**5**, **11**) were readily obtained after treatment of the indole (**3** or **9**) with NaH as base and addition of an excess of dibromoalkane followed by column chromatography purification. The imidazole products (**6**, **7**, **12** and **13**) were obtained in good yield on reacting the indole bromoalkyl derivatives (**4**, **5**, **10** and **11**) with sodium hydride in DMF followed by reaction with imidazole at 45 ^{o}C overnight (Scheme 1).

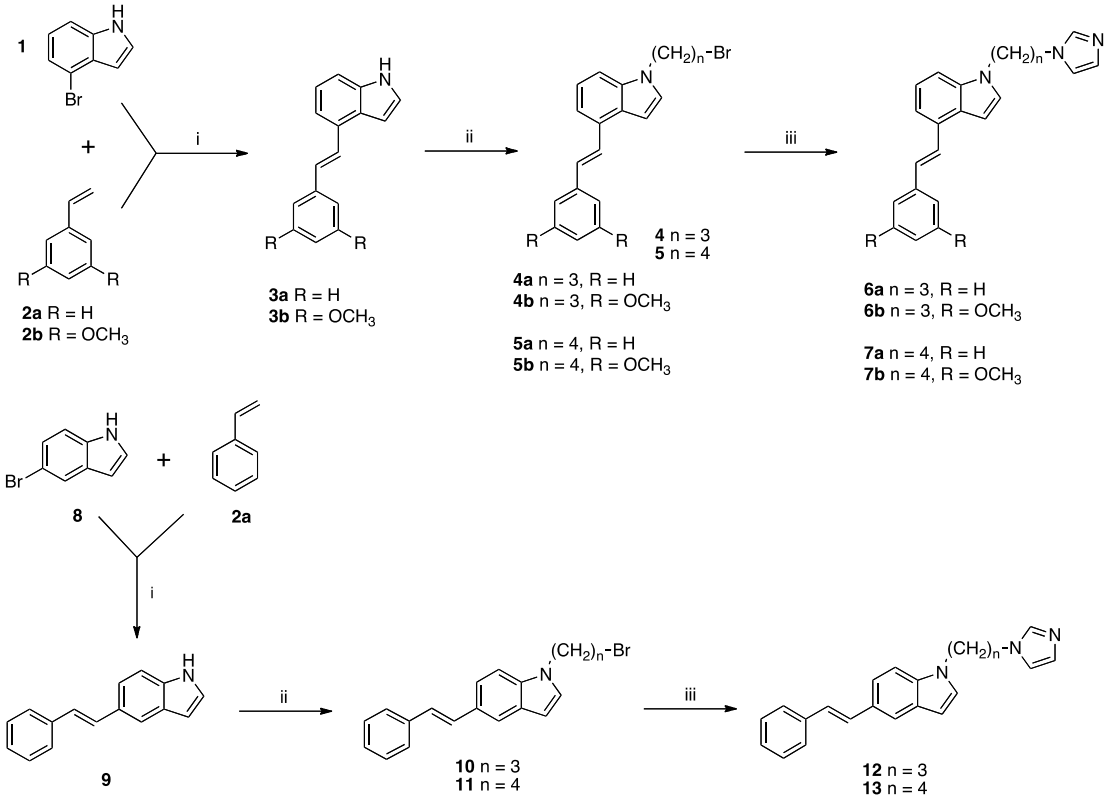

Scheme 1. *Reagents and Conditions*: (i) $Pd(OAc)_2$, ToP, Et_3N, 110 ^oC, 20 h (ii) NaH, DMF, 1,3-dibromopropane or 1,4-dibromobutane, 5 min (iii) NaH, DMF, imidazole, 45 °C, 1 h then r.t. overnight.

Preparation of the indole sulfonamides (**18** and **19**) commenced from the the indole bromoalkyl derivatives (**4** and **5**) (Scheme 2). The bromide was displaced with azide on treatment with sodium azide and the resulting indole alkylazide derivatives (**14** and **15**) reduced via a Staudinger reaction [25] using triphenylphosphine to give the indole alylamines (**16** and **17**). The final step to prepare the indole sulfonamides (**18** and **19**) invovled reaction of the amines (**16** and **17**) with *p*-toluenesulfonyl chloride at 0 ^oC for 30 min in the presence of triethylamine.

To include a compound for testing with a sulfinate bond, 1-(3-benzenesulfonyl-propyl)-4-styryl-1*H*-indole (**20**) was prepared on reaction with bromide (**4a**, n = 3, R = H) with benzene sulfinic acid sodium salt following described methodology (Scheme 2) [26], [27].

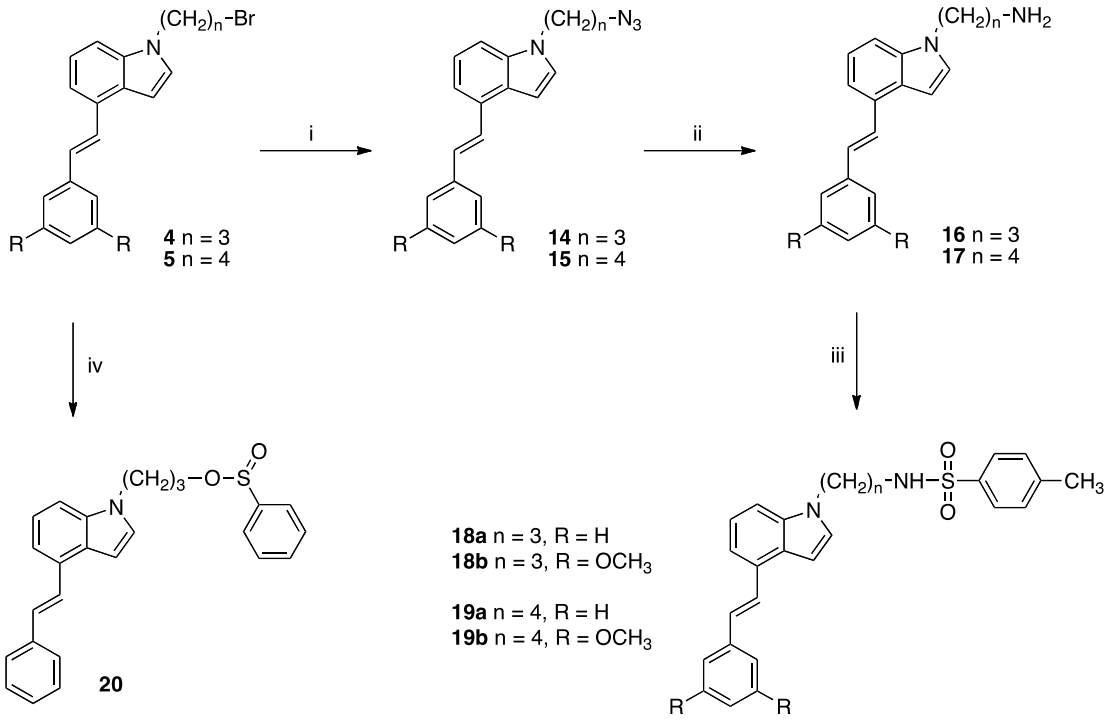

Scheme 2. *Reagents and Conditions*: (i) NaN_3, DMF, r.t., 5 h (ii) (a) PPh_3, THF, r.t. 1h (b) H_2O, 60 ^oC, 2h (iii) TsCl, Et_3N, CH_2Cl_2, 0 °C, 30 min (iv) $C_6H_5SO_2Na$, DMF, r.t., 24 h.

The indole sulfonates (**23**) were prepared in three steps from the indole styrene (**3**) with introduction of the lateral alcohol chain achieved on reaction of **3** with sodium hydride and ethyl-3-bromopropionate and subsequent reduction of the ester (**21**) to the alcohol (**22**) with $LiAlH_4$. The final sulfonates (**23**) were readily prepared by reaction of the alcohols (**22**) with *p*-toluenesulfonyl chloride at room temperature for 24 h in the presence of 4-dimethylaminopyridine (DMAP) (Scheme 3).

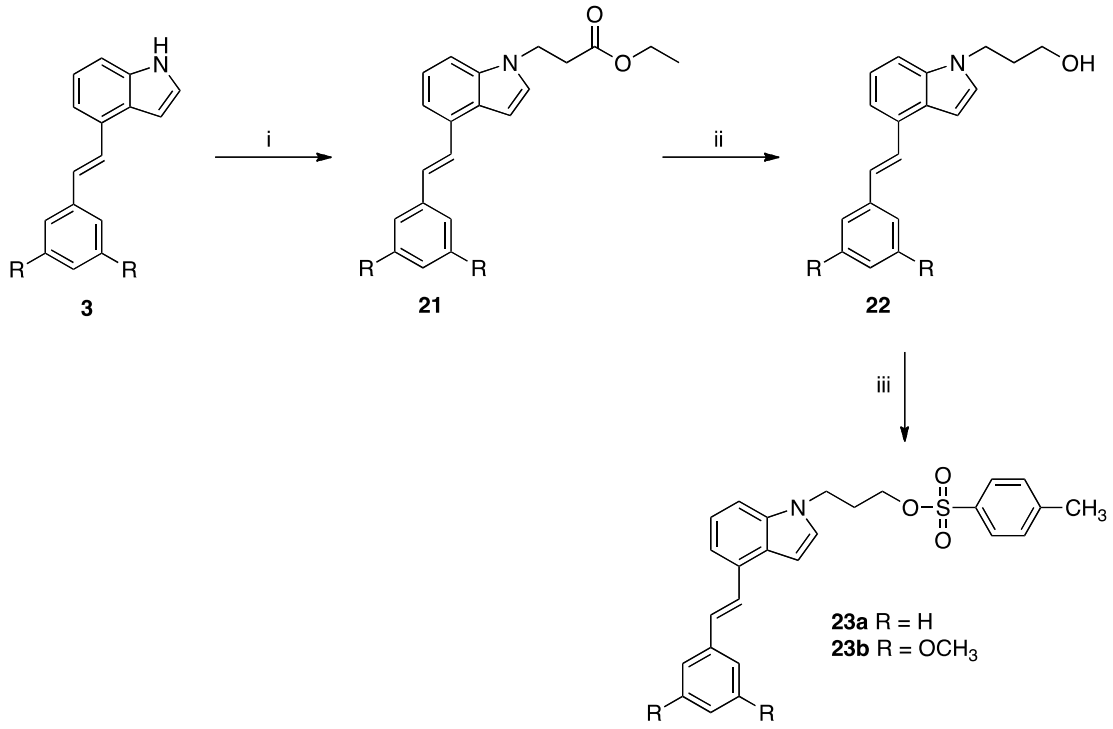

Scheme 3. *Reagents and Conditions*: (i) NaH, DMF, ethyl-3-bromopropionate, 0 °C to r.t., 2 h (ii) $LiAlH_4$, THF, 0 °C 1 h then r.t. 4 h (iii) TsCl, DMAP, CH_2Cl_2, pyridine, r.t., 24 h.

2.2 CYP24A1 Enzyme Inhibition

The CYP24A1 enzymatic assay followed methodology previously described [23], in short human CYP24A1 with an N-terminal fusion to maltose binding protein (MBP) was overexpressed in *Escherichia coli* and purified to homogeneity. The hydrolase enzyme was reconstituted *in vitro*, and the resulting cell-free assay system applied in the screening of the compounds to measure K*i* and IC_{50} (Table 1).

The imidazole styryl indole derivatives **6**, **7**, **12** and **13** were all potent inhibitors of CYP24A1 (K*i* 14-37 nM, IC_{50} 0.19-0.52 μM) with activity comparable with or greater than the standard ketoconazole (K*i* 33 nM, IC_{50} 0.47 μM) (Table 1). The 4-styryl dreivatives with the 4-carbon lateral chain (**7**) were more active than the 3-carbon chain derivatives (**6**), which were of equivalent inhibitory activity to the 5-

styryl derivates (**12** and **13**). Substitution of the styryl aromatic ring (R = H or OCH_3) did not affect the inhibitory activity.

Table 1. IC_{50} and K_i data for indole imidazole and sulfonyl derivatives *vs* CYP24A1

Compound	IC_{50} (μM)	K_I (μM)
6a	0.36	0.026 ± 0.004
6b	0.44	0.031 ± 0.004
7a	0.20	0.014 ± 0.002
7b	0.19	0.014 ± 0.002
12	0.52	0.037 ± 0.004
13	0.52	0.037 ± 0.002
18a	4.8	0.34 ± 0.02
18b	10.4	0.73 ± 0.18
19a	3.3	0.23 ± 0.06
19b	10.5	0.74 ± 0.03
20	7.6	0.54 ± 0.07
23a	9.0	0.64 ± 0.09
23b	16.9	1.19 ± 0.43
Ketoconazole	0.47	0.035

The sulfonyl and sulfinyl derivatives (**18**, **19**, **20** and **23**) displayed reduced CYP24A1 inhibitory activity compared with the standard ketoconazole (Table 1). In this series the substitution of the styryl aromatic ring (R = H or OCH_3) did have an effect with the unsubstituted derivatives (**18a**, **19a**, **20** and **23a**) displaying greater inhibitory activity than the dimethoxy derivatives (**18b**, **19b** and **23b**).

2.3 CYP27B1 Enzyme Inhibition and Selectivity

Inhibition assay of CYP27B1 was performed in a similar way to the CYP24A1 assay as previously described [23], and the resulting cell-free assay system applied in the screening of the compounds to measure K*i* and IC_{50} (Table 2). Compounds with good binding and inhibitory activity against CYP24A1 also displayed similar properties against CYP27B1. A small selectivity was observed for CYP24A1 with the indole imidazole with a lateral four carbon chain (**7a**) displaying

the best selectivity (selectivity CYP27B1/CYP24A1 = 1.8) comparable with the standard, ketoconazole (selectivity CYP27B1/CYP24A1 = 1.7), although two of the derivatives in this series (**6b** and **13**) showed a small selectivity for CYP27B1.

Table 2. IC_{50} and K_i of indole imidazole derivatives vs CYP24A1 and CYP27B1 and selectivity data.

	CYP24A1		CYP27B1		Selectivity
Compound	IC_{50} (μM)	K_I (μM)	IC_{50} (μM)	K_I (μM)	K_I (CYP27B1/ CYP24A1)
6a	0.36	0.026 ± 0.004	0.21	0.034 ± 0.005	1.3
6b	0.44	0.031 ± 0.004	0.14	0.022 ± 0.004	0.71
7a	0.20	0.014 ± 0.002	0.15	0.025 ± 0.003	1.8
7b	0.19	0.014 ± 0.002	0.10	0.017 ± 0.004	1.2
12	0.52	0.037 ± 0.004	0.28	0.046 ± 0.004	1.2
13	0.52	0.037 ± 0.002	0.15	0.024 ± 0.005	0.65
Ketoconazole	0.47	0.033	0.36	0.058	1.7

3. Discussion

The indole-imidazole derivatives were prepared using a 4-step synthetic pathway. The six compounds (**6a**, **6b**, **7a**, **7b**, **12** and **13**, Table 1) showed a very interesting activity in the CYP24A1 enzymatic assay, which is comparable to our (*E*)-*N*-(2-(1*H*-imidazol-1-yl)-2-phenylethyl)-4-styrylbenzamides family previously reported [28]. The inhibition assay would suggest that the length of the lateral chain and position of the styrene on the indole ring are important to activity. The 3 carbon derivatives have lower activity, whereas the introduction of an extra carbon on the lateral chain results in an increase in inhibitory activity up to 2-fold. Substituting a 5-indole as the central core instead of the 4-indole results in a decrease in inhibitory activity.

In order to provide a rational explanation for the observed enzymatic data, flexible alignment and molecular docking studies were performed using MOE 2010 [29] and LeadIT2.1.2 [30]. All the molecular modeling studies were performed using a CYP24A1 homology model built using a rat CYP24A1 crystal structure [31] as a

template and the amino acid sequence of the human isoform following a previous published homology model technique [32]. After performing a molecular docking of the most promising inhibitor (**24**: IC_{50} = 0.11 μM; K*i* = 7.8 nM; CYP24A1/CYP27B1 selectivity = 3.3) from the previously reported (*E*)-*N*-(2-(1*H*-imidazol-1-yl)-2-phenylethyl)-4-styrylbenzamides [28] in the enzyme active site (Figure 2), its active binding conformation pose was kept rigid while a flexible alignment was executed using a database of the six indole-imidazole derivatives.

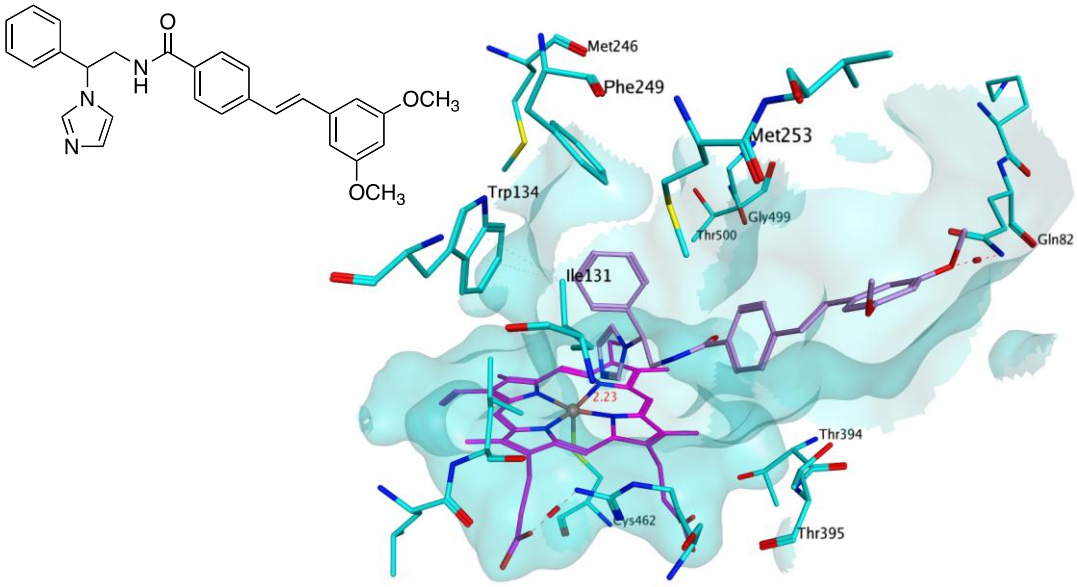

Figure 2. Structure and Docking of **24**: the compound occupies the access tunnel with the imidazole ring in an optimal orientation for the interaction with the iron. The hydrogen bond between the 3-methoxy group and Gln82 stabilises the molecule in a favourable active conformation.

Flexible alignment is a technique which allows determination of the best alignment in terms of internal strain and overlap of different molecular features (*e.g.*: aromatic features, H-bond donors/acceptors, *etc*.) [33]. Using this molecular modeling tool the

alignment of the indole-imidazole derivatives with the **24** binding pose conformation were evaluated and an interesting relation was found between the flexible alignment results (see Table 3) and the enzymatic inhibition assay data. The most active compound in the series, **7b**, presents 4 carbons in the lateral chain and the 4-indole as central core. Figure 3A, shows the alignment between **7b** (yellow) and **24** (lilac).

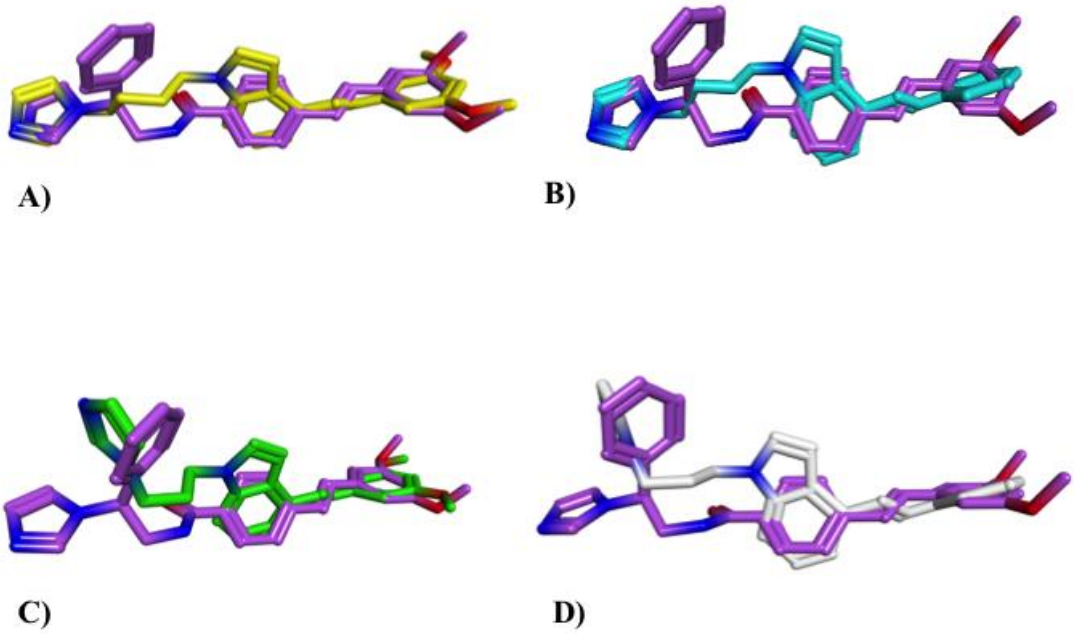

Figure 3: Flexible alignment between **24** (lilac) and (A) **7b** (yellow), (B) **7a** (light blue), (C) **6b** (green), (D) **6a** (white).

The imidazole, the 3,5-dimethoxy phenyl ring and the benzyl portion of the indole core of **7b** overlap perfectly with the corresponding groups of **24**, with **7b** perfectly spatially aligned with our reference compound. Moreover, as reported in Table 4, this conformation has the lowest S value (sum of the internal energy of the ligand [U] and the similarity score [F]) and therefore is the best in terms of overlapping score. The low S value is due to the good internal energy of the ligand pose (U value) and the high similarity score (F value) meaning that the **7b** conformation obtained is not

forced in the first case and that the two molecules have a high shape/functional group similarity in the second case.

Table 3. Scoring results from flexible alignment

Entry	mol	U (kcal/mol)	F	S	dU
1	**7b**	34.3428	-169.6129	-135.2701	0.0
2	**7a**	26.3473	-153.5406	-127.1933	0.0
3	**6b**	32.7516	-148.6960	-115.9444	0.0
4	**6a**	25.0259	-131.2711	-106.2452	0.0
5	**13**	24.4710	-125.4641	-100.9931	0.0
6	**12**	23.3696	-119.7692	-96.4266	0.0

Similar observations can be observed for **7a** (light blue), a 4-indole derivative with 4 lateral chain carbons but with no substituent on the aromatic ring. The compound overlaps perfectly with **24** (Figure 3B) and its S value is the second in the ranking. The absence of the 3,5-dimethoxy substituents results in a decrease in the similarity score F with **24** leading to a slightly higher S value.

The 3 carbons derivatives **6b** (green) and **6a** (white), present a higher S value as a consequence of the unfavorable visual overlapping (Figure 3C and 3D respectively). Both compounds due to the shorter lateral chain do not perfectly overlap with **24** especially in the imidazole ring moiety. The difference in alignment with inhibitor **24** between the 4 carbon and the 3 carbon derivatives could be a plausible explanation for the CYP24A1 enzymatic assay results. **7b** and **7a** overlap better with **24** and this can influence their disposition in the enzyme active site. The docking studies performed confirmed the importance of the length of the lateral chain. All the compounds reach the enzyme active site through the vitamin D access tunnel and are exposed to multiple hydrohobic residues (Ile131, Trp134, Met246, Phe249, Thr394,

Thr395, Gly499, Tyr500*)* which have been reported to have multiple hydrophobic interactions with calcitriol [31]. This disposition allows the imidazole ring to be optimally positioned for the interaction between its nitrogen lone pair and the haem iron. **7b** is disposed in the active site in the same manner as **24**, occupies the full length of the enzyme channel and forms a H-bond between its 3-methoxy group and Gln82 as found for our reference compound (Figure 4).

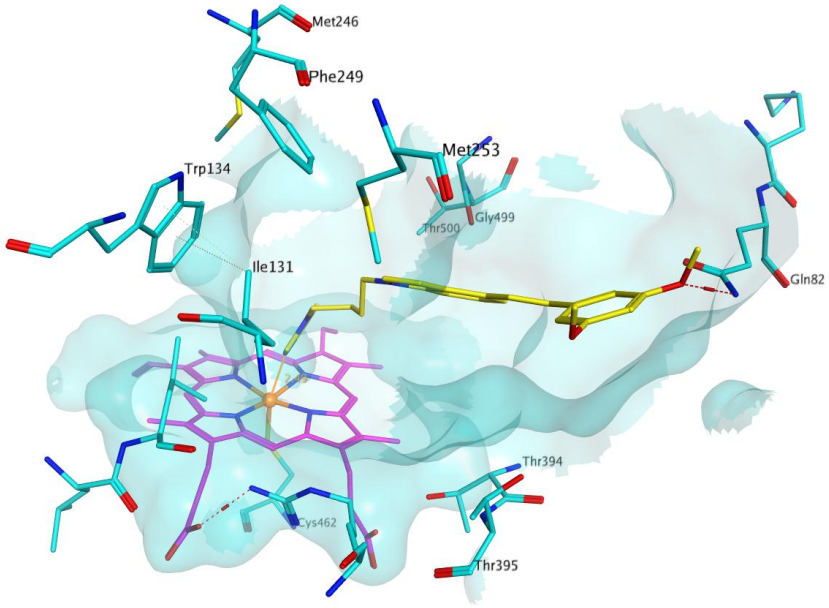

Figure 4: Docking of **7b**: the compound is able to entirely occupy the active site thanks to the 4-carbon lateral chain

Docking studies of **6b** and **6a**, showed the two molecules orientated in the right position with the imidazole ring perpendicular to the iron, but due to the lack of one carbon on the lateral chain they are not able to entirely occupy the active site (far from Gln 82) and their interaction with the CYP24A1 could be less strong than the 4-carbon lateral chain derivatives influencing their inhibition activity (Figure 5).

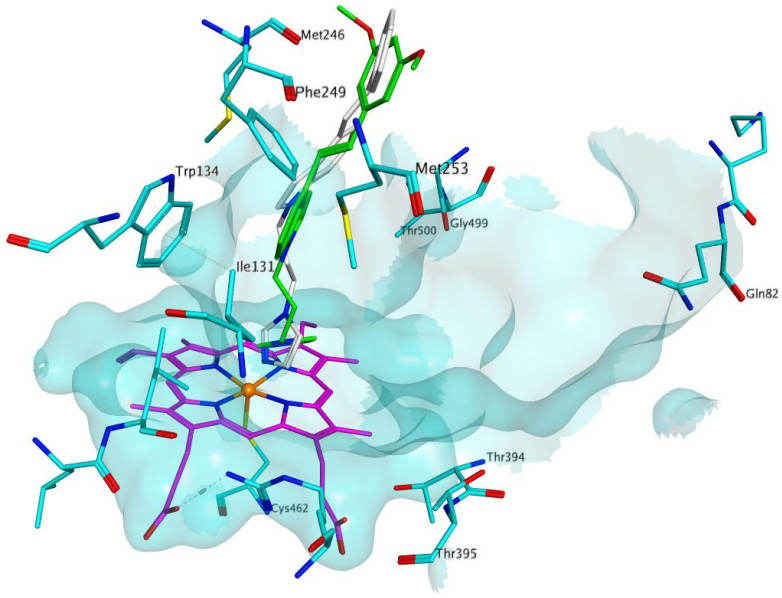

Figure 5. Docking of **6b** and **6a**: the compounds are not able to entirely occupy the active site access tunnel as consequence of the shorter lateral chain.

The 5-indole derivatives **13** (green) and **12** (red) showed the lowest activity among this indole-imidazole series. The flexible alignment results showed both molecules do not completely overlap with **24** (Figure 6) especially in the important imidazole ring region giving a low S value as a final score.

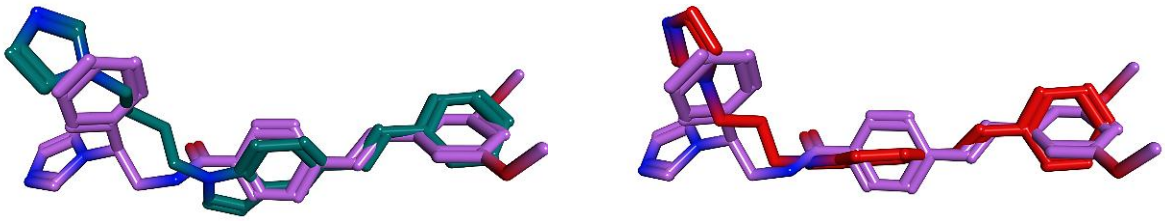

Figure 6: Flexible alignment between **24** (lilac) and **13** (green) and **12** (red): no optimal spatial overlapping was found in the imidazole ring region.

The docking studies of these two derivatives confirmed our initial deduction and the possible connection between the spatial alignment with **24** and the capacity to entirely sit in the enzyme active site. **13** was not able to occupy the active site due to its

structural flexibility conferred by the presence of the stryryl ring in position 5 instead of 4 (Figure 7). As previously mentioned, the inability to accommodate the entire active site can result in a decrease of CYP24A1 enzymatic inhibition.

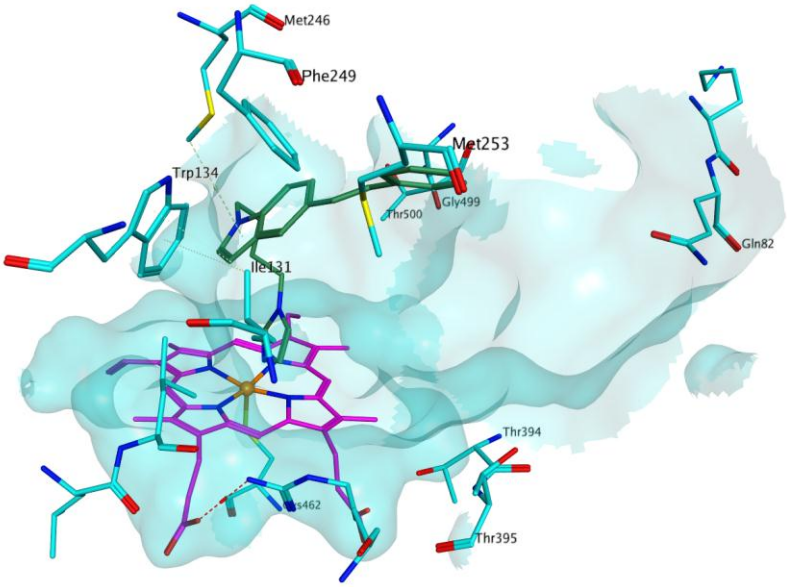

Figure 7. Docking of **13**: the molecule does not occupy entirely the active site due to its structural flexibility conferred by the styryl ring in position 5 of the central indole core.

The replacement of the imidazole in both the indole-sulfonate and indole-sulfonamide series resulted in a notable decrease in inhibitory activity. These results underline the key role of the imidazole ring in the binding to the CYP24A1 haem group [34], [35]. In fact, the higher structural similarity among these three families suggests that the decrease in activity in these two last series of compounds is a consequence of the replacement of the imidazole by the sulfonate or sulfonamide moiety. The interaction of the indole-sulfonate and the indole-sulfonamide derivatives with the haem iron is not strong enough resulting in reduced inhibitory activity. A rational explanation could be found in the different availability of the electron lone pair of the imidazole nitrogen in one case and of the sulfonyl-sulfonamidic oxygen in the other case. The

imidazole lone pair could be more available for the interaction with the haem group making the imidazole-Fe a strong interaction. On the other hand, the possibility to share the lone pair between the two oxygen atoms of the sulfonyl-sulfonamide group makes the oxygen-Fe interaction weaker resulting in the important decrease of the CYP24A1 inhibitory activity. The use of the more stable sulfonamide instead of the sulfonte group gave the desired result with activity improved by 2-3 fold but not comparable with the indole-imidazole family.

4. Conclusions

We have developed methods for the preparation of novel styrylindoles (imidazole, sulfonate and sulfonamide series). The thirteen new styrylindoles have been assayed for the inhibition of CYP24A1 and CYP27B1. The imidazole styrylindoles were the most potent CYP24A1 inhibitors with IC_{50} values from 0.19 - 0.52 μM comparable with the CYP inhibitor ketoconazole (IC_{50} 0.47μM). The sulfonate and sulfonamides displayed only weak CYP24A1 inhibitory activity indicating the importance of the imidazole azole group in interacting with the active site haem moiety. A four carbon lateral chain was optimal resulting in complete occupation of the vitamin D access tunnel and allowing exposure to multiple hydrophobic binding interactions and optimal conformation for the interaction of the imidazole nitrogen lone pair and the active site haem. A small selectivity for CYP24A1 over CYP27B1 comparable with ketoconazole (CYP27B1/CYP24A1 **7a** = 1.8, ketoconazole = 1.7) was observed.

The challenge in the development of CYP24A1 inhibitors is achieving selectivity between CYP24A1 and CYP27B1. In the absence of an available crystal structure of CYP27B1 it is essential to develop a reliable homology model to allow exploitation of any differences between the active sites of CYP24A1 and CYP27B1, however with

the similarity of the two substrates, 1,25$(OH)_2D_3$ and 25(OH) D_3 respectively, any differences are likely to be subtle. This is the current focus of our investigations using the styrylindoles (e.g. **7a**) and styrylbenzamides (e.g. **24**) as lead compounds for further development.

5. Experimental

5.1. Materials and Methods

1,25$(OH)_2D_3$ and 25$(OH)D_3$ were purchased from SAFC-Pharma (Madison, WI). Human MBP-CYP24A1, mouse CYP27B1, bovine adrenodoxin (Adx), and adrenodoxin reductase (AdR) were purified as described previously [14]. All solvents used for chromatography were HPLC grade from Fisher Scientific (UK).

^1H and ^{13}C NMR spectra were recorded with a Bruker Avance DPX500 spectrometer operating at 500 and 125 MHz, with Me_4Si as internal standard. Mass spectra were determined by the EPSRC mass spectrometry centre (Swansea, UK). Flash column chromatography was performed with silica gel 60 (230-400mesh) (Merck) and TLC was carried out on precoated silica plates (kiesel gel 60 F_{254}, BDH). Compounds were visualised by illumination under UV light (254 nm) or by the use of vanillin stain followed by charring on a hotplate. Melting points were determined on an electrothermal instrument and are uncorrected. All solvents were dried prior to use and stored over 4Å molecular sieves, under nitrogen. All compounds were more than 95% pure.

5.1.1 General method for the preparation of styryl-1*H*-indoles 3 and 9. Styrene (**2a**) or 1,3-dimethoxy-5-vinylbenzene (**2b**) (10 mmol), 4-bromoindole (**1**) or 5-bromoindole (**8**) (10 mmol), and triethylamine (20 mmol) were heated in the presence

of tri(*o*-tolylphosphine) (TOP, 0.3 mmol) and palladium (II) acetate (0.05 mmol) in a sealed glass tube at 110°C for 5 h. On completion, water (10 mL) was added. The product was portioned between CH_2Cl_2 (100 mL) and water (100 mL), then the organic layer was dried over $MgSO_4$ and the solvent evaporated under vacuum. The product was isolated by flash column chromatography (petroleum ether-EtOAc 100:0 v/v increasing to 90:10 v/v).

5.1.1.1. 4-Styryl-1*H*-indole (3a, R = H). Obtained in 80% yield as a green solid. M.p. 126-128 ^{o}C. TLC (7:3 Petroleum ether/EtOAc, R*f* = 0.57). ^{1}H NMR ($CDCl_3$): δ 8.30 (bs, 1H, NH), 7.63 (d, *J* = 8.2 Hz, 2H, Ar), 7.59 (d, *J* = 16.3 Hz, 1H, alkene), 7.33 (d, *J* = 7.4 Hz, 2H, Ar), 7.30 (d, *J* = 16.1 Hz, 1H, alkene), 7.20-7.26 (m, 4H, Ar and indole), 7.03 (m, 1H, Ar), 6.72 (s, 1H, indole). ^{13}C NMR ($CDCl_3$): δ□136.8, 135.1, 128.6, 125.1 (C, Ar), 128.2, 127.5, 126.3, 126.2, 125.4, 121.6, 119.3, 113.6, 109.5, 100.0 (CH, Ar and alkene). Anal. Calcd for $C_{16}H_{13}N$ $0.1H_2O$ (221.08692): C, 86.92; H, 6.02; N, 6.34. Found: C, 87.10; H, 5.86; N, 6.40.

5.1.1.2. 4-(3,5-Dimethoxystyryl)-1*H*-indole (3b, R = OCH_3). Obtained in 65% yield as a green-grey solid. M.p. 96-98 ^{o}C. TLC (7:3 Petroleum ether/EtOAc, R*f* = 0.50). ^{1}H NMR ($CDCl_3$): δ 8.27 (bs, 1H, NH), 7.53 (d, *J* = 16.3 Hz, 1H, alkene), 7.39 (d, *J* = 7.3 Hz, 1H, Ar), 7.36 (d, *J* = 8.1 Hz, 1H, Ar), 7.31 (t, *J* = 2.9 Hz, 1H, indole), 7.23-7.28 (m, 2H, Ar and alkene), 6.87 (m, 1H, indole), 6.78 (d, *J* = 2.2 Hz, 2H, Ar), 6.45 (t, *J* = 2.2 Hz, 1H, Ar), 3.88 (s, 6H, 2 x OCH_3). ^{13}C-NMR ($CDCl_3$): δ 161.0 (C), 140.0, 136.2, 129.5, 126.3 (C, Ar), 129.3, 127.9, 124.4, 122.2, 117.7, 110.6, 104.6, 101.3, 99.7 (CH, Ar and alkene), 55.4 (2 x OCH_3). EI-HRMS $(M + H)^+$ found 280.1332, calculated for $C_{18}H_{18}NO_2$ 280.1335.

5.1.1.3. 5-Styryl-1*H*-indole (9). Obtained in 49% yield as a pale green solid. M.p. 152-154 ^{o}C. TLC (7:3 Petroleum ether/EtOAc, R*f* = 0.62). ^{1}H NMR ($CDCl_3$): δ 8.15

(bs, 1H, NH), 7.80 (s, 1H, Ar), 7.57 (d, J = 7.4 Hz, 2H, Ar), 7.49 (dd, $J_{x,a}$ = 1.7 Hz, $J_{x,b}$ = 8.7 Hz, 1H, Ar_x), 7.37-7.41 (m, 3H, Ar and indole), 7.25-7.31 (m, 2H, Ar and alkene), 7.23 (t, J = 2.8 Hz, 1H, Ar), 7.12 (d, J = 16.3 Hz, 1H, alkene), 6.60 (m, 1H, indole). ^{13}C-NMR ($CDCl_3$): δ 138.0, 135.6, 129.6, 128.2 (C, Ar), 13.0, 128.6, 126.9, 126.2, 126.1, 124.7, 120.7, 119.5, 111.2, 103.0 (CH, Ar and alkene). Anal. Calcd for $C_{16}H_{13}N$ 0.1H_2O (221.08692): C, 86.92; H, 6.02; N, 6.34. Found: C, 87.07; H, 6.28; N, 6.44.

5.1.2 General method for the preparation of styryl-1-bromoalkyl-1*H*-indoles 4, 5, 10 and 11. The different 4/5-(3,5-unsubstituted/substituted styryl)-1*H*-indole (**3** or **9**) (7 mmol) and NaH (60% dispersion in mineral oil) (21 mmol) in dry DMF (10 mL) were cooled to 0˚C using an ice bath and stirred for 5 min. 1,3-Dibromopropane or 1,4-dibromobutane (70 mmol) was added and the reaction mixture was stirred for 10 min. On completion, the solvent was evaporated under reduced pressure and the residue was dissolved in CH_2Cl_2 (100 mL), washed with water (2 x 50 mL) and dried over $MgSO_4$. The organic layer was then evaporated to dryness and the residue was purified by flash column chromatography to obtain the pure product.

5.1.2.1. 1-(3-Bromopropyl)-4-styryl-1*H*-indole (4a, R = H). Purified by flash column chromatography eluting with petroleum ether-diethyl ether 100:0 v/v increasing to 99:1 v/v. Obtained in 50% yield as a thick yellow oil. TLC (3:1 Petroleum ether/EtOAc, R*f* = 0.73). ^{1}H NMR ($CDCl_3$): δ 7.61 (d, J = 7.3 Hz, 2H, Ar), 7.55 (d, J = 16.3 Hz, 1H, alkene), 7.39-7.43 (m, 3H, Ar), 7.26-7.36 (m, 4H, Ar and alkene), 7.25 (d, J = 3.0 Hz, 1H, indole), 6.83 (d, J = 3.0 Hz, 1H, indole), 4.40 (t, J = 6.4 Hz, 2H, CH_2), 3.34 (t, J = 6.1 Hz, 2H, CH_2), 2.39 (m, 2H, CH_2). ^{13}C-NMR ($CDCl_3$): δ 137.9, 136.3, 130.1, 129.9 (C, Ar), 129.5, 128.6, 128.3, 127.4, 127.1,

126.5, 121.9, 117.3, 108.7, 100.1 (CH, Ar and alkene), 44.1, 32.7, 30.4 (CH_2). EI-HRMS $(M + H)^+$ found 341.07795, calculated for $C_{19}H_{19}BrN$ 341.07791.

5.1.2.2. 4-(3,5-Dimethoxystyryl)-1-(3-bromopropyl)-1*H*-indole (4b, R = OCH_3). Purified by flash column chromatography eluting with petroleum ether-EtOAc 100:0 v/v increasing to 95:5 v/v. Obtained in 66% yield as a yellow oil. TLC (3:1 Petroleum ether/EtOAc, R*f* = 0.72). ^{1}H NMR ($CDCl_3$): δ 7.53 (d, *J* = 16.3 Hz, 1H, alkene), 7.39 (d, *J* = 7.3 Hz, 1H, Ar), 7.34 (d, *J* = 8.1 Hz, 1H, Ar), 7.23-7.28 (m, 3H, Ar, indole and alkene), 6.83 (m, 1H, indole), 6.77 (d, *J* = 2.3 Hz, 2H, Ar), 6.44 (t, *J* = 2.3 Hz, 1H, Ar), 4.38 (t, *J* = 6.3 Hz, 2H, CH_2), 3.88 (s, 6H, 2 x OCH_3), 3.34 (t, *J* = 6.1 Hz, 2H, CH_2), 2.39 (m, 2H, CH_2). ^{13}C-NMR ($CDCl_3$): δ 161.0 (C), 140.0, 136.3, 129.9, 127.1 (C, Ar), 129.4, 128.3, 127.7, 121.9, 117.4, 108.8, 104.6, 101.1, 99.7 (CH, Ar and alkene), 55.4 (2 x OCH_3). EI-HRMS $(M + H)^+$ found 400.0911, calculated for $C_{21}H_{23}BrNO_2$ 400.0907.

5.1.2.3. 1-(4-Bromobutyl)-4-styryl-1*H*-indole (5a, R = H). Purified by flash column chromatography eluting with petroleum ether-EtOAc 100:0 v/v increasing to 90:10 v/v. Obtained in 86% yield as a thick yellow oil. TLC (3:1 Petroleum ether/EtOAc, R*f* = 0.73). ^{1}H NMR ($CDCl_3$): δ 7.64 (d, *J* = 7.4 Hz, 2H, Ar), 7.58 (d, *J* = 16.2 Hz, 1H, alkene), 7.42-7.45 (m, 3H, Ar), 7.30-7.37 (m, 4H, Ar and alkene), 7.19 (d, *J* = 3.3 Hz, 1H, indole), 6.85 (d, *J* = 3.3 Hz, 1H, indole), 4.21 (t, *J* = 6.7 Hz, 2H, CH_2), 3.41 (t, *J* = 6.5 Hz, 2H, CH_2), 2.06 (m, 2H, CH_2), 1.89 (m, 2H, CH_2). ^{13}C-NMR ($CDCl_3$): δ 138.0, 136.4, 130.0, 127.4 (C, Ar), 129.4, 128.7, 128.1, 127.5, 127.0, 126.5, 121.8, 117.2, 108.7, 99.9 (CH, Ar and alkene), 45.6, 32.9, 29.9, 28.8 (CH_2). EI-HRMS $(M + H)^+$ found 354.0857, calculated for $C_{20}H_{21}BrN$ 354.0852.

5.1.2.4. 4-(3,5-Dimethoxystyryl)-1-(4-bromobutyl)-1*H*-indole (5b, R = OCH_3). Purified by flash column chromatography eluting with petroleum ether-EtOAc 100:0

v/v increasing to 90:10 v/v. Obtained in 69% yield as a thick yellow oil. TLC (3:1 Petroleum ether/EtOAc, R*f* = 0.55). ^{1}H NMR ($CDCl_3$): δ 7.51 (d, *J* = 16.4 Hz, 1H, alkene), 7.38 (d, *J* = 7.3 Hz, 1H, Ar), 7.30 (d, *J* = 8.0 Hz, 1H, Ar), 7.22-7.31 (m, 2H, Ar and alkene), 7.18 (d, *J* = 3.2 Hz, 1H, indole), 6.82 (d, *J* = 3.2 Hz, 1H, indole), 6.77 (d, *J* = 2.2 Hz, 2H, Ar), 6.44 (t, *J* = 2.2 Hz, 1H, Ar), 4.21 (t, *J* = 6.8 Hz, 2H, CH_2), 3.88 (s, 6H, 2 x OCH_3), 3.40 (t, *J* = 6.6 Hz, 2H, CH_2), 2.06 (m, 2H, CH_2), 1.89 (m, 2H, CH_2). ^{13}C-NMR ($CDCl_3$): δ 161.0 (C), 140.0, 136.4, 129.8, 127.0 (C, Ar), 129.3, 127.9, 127.7, 121.8, 117.3, 108.8, 104.6, 99.8, 99.7 (CH, Ar and alkene), 55.4 (2 x OCH_3), 45.6, 32.9, 29.9, 28.8 (CH_2). EI-HRMS $(M)^+$ found 413.0990, calculated for $C_{22}H_{24}BrNO_2$ 413.0985.

5.1.2.5. 1-(3-Bromopropyl)-5-styryl-1*H*-indole (10). Purified by flash column chromatography eluting with petroleum ether-diethyl ether 100:0 v/v increasing to 99:1 v/v. Obtained in 46% yield as a white solid. M.p. 78-80 ^{o}C. TLC (9:1 Petroleum ether/EtOAc, R*f* = 0.50). ^{1}H NMR ($CDCl_3$): δ 7.78 (s, 1H, Ar), 7.56 (d, *J* = 7.2 Hz, 2H, Ar), 7.50 (dd, $J_{x,a}$ = 1.6 Hz, $J_{x,b}$ = 8.6 Hz, 1H, Ar_x), 7.37-7.42 (m, 3H, Ar), 7.23-7.30 (m, 2H, Ar and alkene), 7.17 (d, *J* = 3.1 Hz, 1H, indole), 7.11 (d, *J* = 16.3 Hz, 1H, alkene), 6.54 (d, *J* = 3.2 Hz, 1H, indole), 4.36 (t, *J* = 6.4 Hz, 2H, CH_2), 3.34 (t, *J* = 6.1 Hz, 2H, CH_2), 2.39 (m, 2H, CH_2). ^{13}C-NMR ($CDCl_3$): δ 138.0, 135.7, 129.3, 129.1 (C, Ar), 129.9, 128.6, 128.2, 126.9, 126.2, 126.1, 120.3, 119.8, 109.5, 102.0 (CH, Ar and alkene), 44.1, 32.8, 30.4 (CH_2). Anal. Calcd for $C_{19}H_{18}BrN$ (340.256): C, 67.07; H, 5.33; N, 4.11. Found: C, 66.73; H, 5.75; N, 4.08.

5.1.2.5. 1-(4-Bromobutyl)-5-styryl-1*H*-indole (11). Purified by flash column chromatography eluting with petroleum ether-EtOAc 100:0 v/v increasing to 98:2 v/v. Obtained in 84% yield as a yellow wax. TLC (9:1 Petroleum ether/EtOAc, R*f* = 0.44). ^{1}H NMR ($CDCl_3$): δ 7.78 (s, 1H, Ar), 7.56 (d, J = 7.5 Hz, 2H, Ar), 7.50 (dd, $J_{x,a}$ = 1.3

Hz, $J_{x,b}$ = 8.6 Hz, 1H, Ar_x), 7.38-7.42 (m, 2H, Ar), 7.34 (d, J = 8.6 Hz, 1H, Ar) 7.24-7.30 (m, 2H, Ar and alkene), 7.12 (d, J = 16.3 Hz, 1H, alkene), 7.11 (d, J = 3.2 Hz, 1H, indole), 6.54 (d, J = 3.2 Hz, 1H, indole), 4.19 (t, J= 6.9 Hz, 2H, CH_2), 3.41 (t, J= 6.6 Hz, 2H, CH_2), 2.00 (m, 2H, CH_2), 1.89 (m, 2H, CH_2) . ^{13}C-NMR ($CDCl_3$): δ 138.0, 135.8, 129.1, 129.0 (C, Ar), 130.0, 128.6, 128.2, 126.9, 126.2, 126.0, 120.2, 119.8, 109.5, 101.8 (CH, Ar and alkene), 45.6, 32.9, 29.9, 28.8 (CH_2). EI-HRMS $(M + H)^+$ found 354.0849, calculated for $C_{20}H_{21}BrN$ 354.0852.

5.1.3 General method for the preparation of imidazoles 6, 7, 12 and 13. A suspension of NaH (60% dispersion in mineral oil) (6 mmol) in dry DMF (15 mL) was stirred and heated at 60˚C for 5 min. Imidazole (6 mmol) was added and the reaction mixture was heated at 60˚C for 1 h. The reaction mixture was cooled to room temperature and the styryl-1-bromoalkyl-1*H*-indole (**4**, **5**, **10** or **11**) (3 mmol) was added. The reaction mixture was heated at 60˚C overnight and then hydrolysed by adding H_2O (100 mL). The aqueous layer was extracted with EtOAc (3 x 100 mL); the organic layers were collected and dried over $MgSO_4$. The solvent was then evaporated to dryness and the residue was purified by flash column chromatography (petroleum ether-EtOAc 50:50 v/v then CH_2Cl_2-MeOH 100:0 v/v increasing to 98:2 v/v) to obtain the pure desired product.

5.1.3.1. 1-[3-(1*H*-Imidazol-1-yl)propyl]-4-styryl-1*H*-indole (6a, R = H). Obtained in 72% yield as a yellow glue. TLC (9:1 CH_2Cl_2/MeOH, R*f* = 0.31). ^{1}H NMR ($CDCl_3$): δ 7.61 (d, *J* = 7.4 Hz, 2H, Ar), 7.54 (d, *J* = 16.1 Hz, 1H, alkene), 7.48 (s, 1H, imid), 7.39-7.42 (m, 3H, Ar), 7.24-7.34 (m, 4H, Ar and alkene), 7.19 (d, *J* = 8.4 Hz, 1H, Ar), 7.14 (s, 1H, imid), 7.12 (d, *J* = 3.2 Hz, 1H, indole), 6.93 (s, 1H, imid), 6.86 (d, *J* = 3.1 Hz, 1H, indole), 4.17 (t, *J* = 6.6 Hz, 2H, CH_2), 3.91 (t, *J* = 7.0 Hz, 2H,

CH_2), 2.39 (m, 2H, CH_2). ^{13}C-NMR ($CDCl_3$): δ 137.8, 136.3, 130.2, 127.1 (C, Ar), 137.2, 130.0, 129.6, 128.6, 127.7, 127.5, 126.5, 122.1, 118.5, 117.4, 108.5, 102.4, 100.5 (CH, Ar and alkene), 43.8, 43.0, 31.0 (CH_2). EI-HRMS $(M + H)^+$ found 328.1807, calculated for $C_{22}H_{22}N_3$ 328.1808.

5.1.3.2. 1-[3-(1*H*-Imidazol-1-yl)propyl]-4-(3,5-dimethoxystyryl)-1*H*-indole (6b, R = OCH_3). Obtained in 72% yield as a yellow-orange glue. TLC (3:1 Petroleum ether/EtOAc, R*f* = 0.14). ^{1}H NMR ($CDCl_3$): δ 7.51 (d, *J* = 16.3 Hz, 1H, alkene), 7.48 (s, 1H, imid), 7.4 0 (d, *J* = 7.3 Hz, 1H, Ar), 7.19-7.26 (m, 3H, Ar and alkene), 7.14 (s, 1H, imid), 7.12 (d, *J* = 3.1 Hz, 1H, indole), 6.93 (s, 1H, imid), 6.85 (d, *J* = 3.1 Hz, 1H, indole), 6.77 (d, *J* = 2.2 Hz, 2H, Ar), 6.44 (t, *J* = 2.3 Hz, 1H, Ar), 4.17 (t, *J* = 6.7 Hz, 2H, CH_2), 3.91 (t, *J* = 6.8 Hz, 2H, CH_2), 3.88 (s, 6H, 2 x OCH_3), 2.39 (m, 2H, CH_2). ^{13}C-NMR ($CDCl_3$): δ 161.0 (C), 139.9, 136.3, 130.0, 127.5 (C, Ar), 137.2, 129.6, 128.2, 127.8, 122.1, 118.5, 117.6, 108.6, 106.2, 104.6, 100.5, 99.8 (CH, Ar and alkene), 55.4 (2 x OCH_3), 43.8, 43.0, 31.0 (CH_2). EI-HRMS $(M + H)^+$ found 388.2018, calculated for $C_{24}H_{26}N_3O_2$ 388.2020.

5.1.3.3. 1-[4-(1*H*-Imidazol-1-yl)butyl]-4-styryl-1*H*-indole (7a, R = H). Obtained in 67% yield as a thick yellow oil. TLC (9:1 CH_2Cl_2/MeOH, R*f* = 0.40). ^{1}H NMR ($CDCl_3$): δ 7.60 (d, *J* = 7.5 Hz, 2H, Ar), 7.58 (d, *J* = 16.3 Hz, 1H, alkene), 7.38-7.41 (m, 4H, Ar and imid), 7.23-7.33 (m, 5H, Ar, alkene and imid), 7.13 (d, *J* = 3.2 Hz, 1H, indole), 7.06 (s, 1H, imid), 6.82 (d, *J* = 3.2 Hz, 1H, indole), 4.16 (t, *J* = 6.5 Hz, 2H, CH_2), 3.85 (t, *J* = 6.9 Hz, 2H, CH_2), 1.85 (m, 2H, CH_2), 1.78 (m, 2H, CH_2). ^{13}C-NMR ($CDCl_3$): δ 137.9, 136.3, 130.1, 127.0 (C, Ar), 137.0, 129.6, 129.5, 128.6, 127.8, 127.4, 127.1, 126.4, 121.9, 118.6, 117.2, 108.6, 100.1 (CH, Ar and alkene), 46.4, 45.9, 28.6, 27.2 (CH_2). EI-HRMS $(M + H)^+$ found 342.1959, calculated for $C_{23}H_{24}N_3$ 342.1965.

5.1.3.4. 1-[4-(1*H*-Imidazol-1-yl)butyl]-4-(3,5-dimethoxystyryl)-1*H*-indole (7b, R = OCH_3). Obtained in 75% yield as a thick yellow oil. TLC (9:1 CH_2Cl_2/MeOH, R*f* = 0.48). ^{1}H NMR ($CDCl_3$): δ 7.50 (d, J = 16.1 Hz, 1H, alkene), 7.37-7.40 (m, 2H, Ar and imida.), 7.23-7.26 (m, 3H, Ar and alkene), 7.13 (d, *J* = 3.3 Hz, 1H, indole), 7.06 (s, 1H, imid), 6.83 (s, 1H, imid), 6.81 (d, *J* = 3.3 Hz, 1H, indole), 6.76 (d, *J* = 2.2 Hz, 2H, Ar), 6.44 (t, *J* = 2.2 Hz, 1H, Ar), 4.17 (t, *J* = 6.3 Hz, 2H, CH_2), 3.87 (s, 6H, 2 x OCH_3), 3.85 (t, *J* = 6.7 Hz, 2H, CH_2), 1.86 (m, 2H, CH_2), 1.78 (m, 2H, CH_2). ^{13}C-NMR ($CDCl_3$): δ 161.0 (C), 139.9, 136.3, 129.9, 127.9 (C, Ar), 137.0, 129.6, 129.4, 127.6, 127.0, 121.9, 118.6, 117.4, 108.7, 104.6, 100.1, 99.8 (CH, Ar and alkene), 55.4 (2 x OCH_3), 46.4, 45.9, 28.6, 27.2 (CH_2). EI-HRMS $(M + H)^+$ found 402.2173, calculated for $C_{25}H_{28}N_3O_2$ 402.2176.

5.1.3.5. 1-[3-(1*H*-Imidazol-1-yl)propyl]-5-styryl-1*H*-indole (12). Obtained in 83% yield as a white solid. TLC (9:1 CH_2Cl_2/MeOH, R*f* = 0.61). M.p. 116-118 ^{o}C. ^{1}H NMR ($CDCl_3$): δ 7.78 (s, 1H, Ar), 7.56 (d, *J* = 7.3 Hz, 2H, Ar), 7.45-7.52 (m, 2H, Ar), 7.38-7.40 (m, 2H, Ar), 7.22-7.28 (m, 3 H, Ar, imid and alkene), 7.15 (s, 1H, imid), 7.11 (d, *J* = 16.3 Hz, 1H, alkene), 7.04 (d, *J* = 3.1 Hz, 1H, indole), 6.92 (s, 1H, imid), 6.57 (d, *J* = 3.1 Hz, 1H, indole), 4.13 (t, *J* = 6.6 Hz, 2H, CH_2), 3.90 (t, *J* = 6.8 Hz, 2H, CH_2), 2.39 (m, 2H, CH_2). ^{13}C-NMR ($CDCl_3$): δ 137.9, 135.6, 129.5, 129.1 (C, Ar), 137.2, 130.0, 128.6, 128.0, 127.0, 126.3, 126.2, 120.6, 119.9, 118.6, 109.4, 102.4 (CH, Ar and alkene), 43.8, 42.9, 31.0 (CH_2). Anal. Calcd for $C_{22}H_{21}N_3$ $0.5H_2O$ (336.1814): C, 78.59; H, 6.32; N, 12.49. Found: C, 78.56; H, 6.70; N, 12.48.

5.1.3.6. 1-[4-(1*H*-Imidazol-1-yl)butyl]-5-styryl-1*H*-indole (13). Obtained in 67% yield as a white solid. TLC (9:1 CH_2Cl_2/MeOH, R*f* = 0.50). M.p. 114-116 ^{o}C. ^{1}H NMR ($CDCl_3$): δ 7.77 (s, 1H, Ar), 7.55 (d, *J* = 7.5 Hz, 2H, Ar), 7.48 (dd, $J_{x,a}$ = 1.5 Hz, $J_{x,b}$ = 8.6 Hz, 1H, Ar_x), 7.36-7.42 (m, 3H, Ar and alkene), 7.30 (d, *J* = 8.6 Hz, 1H,

Ar), 7.24-7.28 (m, 2H, Ar and imid), 7.10 (d, *J* = 16.3 Hz, 1H, alkene), 7.07 (s, 1H, imid), 7.05 (d, *J* = 3.1 Hz, 1H, indole), 6.84 (s, 1H, imid), 6.53 (d, *J* = 3.1 Hz, 1H, indole), 4.15 (t, *J* = 6.4 Hz, 2H, CH_2), 3.86 (t, *J* = 6.9 Hz, 2H, CH_2), 1.86 (m, 2H, CH_2), 1.79 (m, 2H, CH_2). ^{13}C-NMR ($CDCl_3$): δ 138.0, 135.7, 129.2, 129.0 (C, Ar), 137.0, 129.9, 129.7, 128.6, 128.1, 126.9, 126.2, 126.1, 120.3, 119.9, 118.6, 109.4, 102.0 (CH, Ar and alkene), 46.4, 45.8, 28.6, 27.2 (CH_2). Anal. Calcd for $C_{23}H_{23}N_3$ 0.1H_2O (342.99077): C, 80.54; H, 6.81; N, 12.25. Found: C, 80.39; H, 7.39; N, 12.20.

5.1.4 General method for the preparation of azides 14 and 15. Sodium azide (4.5 mmol) was added to a solution of styryl-1-bromoalkyl-1*H*-indole (**4** or **5**) (3 mmol) in DMF (3 mL). The resulting green reaction mixture was stirred at room temperature for 5 h then H_2O (20 mL) was added and the aqueous layer extracted with EtOAc (3 x 20 mL). The combined organic phase was washed with brine (30 mL), dried over $MgSO_4$ and evaporated *in vacuo* to give the pure product as a glue.

5.1.4.1. 1-(3-Azido-propyl)-4-styryl-1*H*-indole (14a, R = H). Obtained in 82% yield as an orange glue. TLC (4:1 Petroleum ether/EtOAc, R*f* = 0.50). ^{1}H NMR ($CDCl_3$): δ 7.62 (d, *J* = 7.3 Hz, 2H, Ar), 7.55 (d, *J* = 16.4 Hz, 1H, alkene), 7.39-7.43 (m, 3H, Ar), 7.26-7.35 (m, 4H, Ar and alkene), 7.19 (d, *J* = 3.1 Hz, 1H, indole), 6.84 (d, *J* = 3.0 Hz, 1H, indole), 4.29 (t, *J* = 6.6 Hz, 2H, CH_2), 3.29 (t, *J* = 6.4 Hz, 2H, CH_2), 2.12 (m, 2H, CH_2). ^{13}C-NMR ($CDCl_3$): δ 137.9, 136.3, 130.1, 127.0 (C, Ar), 129.5, 128.1, 127.4, 127.1, 126.5, 122.0, 117.3, 108.6, 100.2 (CH, Ar and alkene), 48.3, 43.2, 29.3 (CH_2). EI-HRMS $(M + H)^+$ found 303.1608, calculated for $C_{19}H_{19}N_4$ 303.1604.

5.1.4.2. 1-(3-Azido-propyl)-4-(3,5-dimethoxystyryl)-1*H*-indole (14b, R = OCH_3). Obtained in 72% yield as an orange glue. TLC (4:1 Petroleum ether/EtOAc, R*f* = 0.50). ^{1}H NMR ($CDCl_3$): δ 7.50 (d, *J* = 16.2 Hz, 1H, alkene), 7.36 (d, *J* = 7.2 Hz, 1H,

Ar), 7.21-7.29 (m, 3H, Ar, and alkene), 7.16 (d, J = 3.2 Hz, 1H, indole), 6.81 (dd, $J_{x,a}$ = 0.8 Hz, $J_{x,b}$ = 2.6 Hz, 1H, indole) 6.75 (d, J = 2.2 Hz, 2H, Ar), 6.42 (t, J = 2.2 Hz, 1H, Ar), 4.23 (t, J = 6.7 Hz, 2H, CH_2), 3.85 (s, 6H, 2 x OCH_3), 3.24 (t, J = 6.2 Hz, 2H, CH_2), 2.07 (m, 2H, CH_2). ^{13}C-NMR ($CDCl_3$): δ 161.0 (C), 139.9, 136.3, 129.7, 127.0 (C, Ar), 129.3, 128.2, 127.6, 121.9, 117.4, 108.8, 104.6, 100.4, 99.7 (CH, Ar and alkene), 55.3 (2 x OCH_3), 48.3, 43.1, 29.3 (CH_2). EI-HRMS $(M + H)^+$ found 363.1817, calculated for $C_{21}H_{23}BrN_4O_2$ 363.1816.

5.1.4.3. 1-(4-Azido-butyl)-4-styryl-1*H*-indole (15a, R = H). Obtained in 86% yield as a yellow glue. TLC (4:1 Petroleum ether/EtOAc, R*f* = 0.57). ^{1}H NMR ($CDCl_3$): δ 7.63 (d, J = 7.4 Hz, 2H, Ar), 7.58 (d, J = 16.2 Hz, 1H, alkene), 7.41-7.44 (m, 3H, Ar), 7.35 (d, J = 16.2 Hz, 1H, alkene), 7.26-7.33 (m, 3H, Ar), 7.10 (d, J = 3.1 Hz, 1H, indole), 6.85 (d, J = 3.1 Hz, 1H, indole), 4.18 (t, J = 6.97 Hz, 2H, CH_2), 3.28 (t, J = 6.8 Hz, 2H, CH_2), 1.95 (m, 2H, CH_2), 1.61 (m, 2H, CH_2). ^{13}C-NMR ($CDCl_3$): δ 138.0, 136.4, 130.0, 127.4 (C, Ar), 129.3, 128.7, 128.1, 127.5, 127.0, 126.5, 121.5, 117.2, 108.8, 99.3 (CH, Ar and alkene), 45.6, 32.9, 29.9, 28.8 (CH_2). EI-HRMS $(M + H)^+$ found 317.1764, calculated for $C_{20}H_{21}N_4$ 317.1761.

5.1.4.4. 1-(4-Azido-butyl)-4-(3,5-dimethoxystyryl)-1*H*-indole (15b, R = OCH_3). Obtained in 57% yield as an orange glue. TLC (4:1 Petroleum ether/EtOAc, R*f* = 0.34). ^{1}H NMR ($CDCl_3$): δ 7.51 (d, J = 16.2 Hz, 1H, alkene), 7.38 (d, J = 7.1 Hz, 1H, Ar), 7.23-7.30 (m, 3H, Ar and alkene), 7.18 (d, J = 3.3 Hz, 1H, indole), 6.82 (d, J = 3.1 Hz, 1H, indole), 6.77 (d, J = 2.2 Hz, 2H, Ar), 6.44 (t, J = 2.2 Hz, 1H, Ar), 4.21 (t, J = 6.8 Hz, 2H, CH_2), 3.88 (s, 6H, 2 x OCH_3), 3.30 (t, J = 6.7 Hz, 2H, CH_2), 1.97 (m, 2H, CH_2), 1.62 (m, 2H, CH_2). ^{13}C-NMR ($CDCl_3$): δ 161.0 (C), 140.0, 136.4, 129.8, 127.0 (C, Ar), 129.3, 127.9, 121.8, 117.3, 108.8, 104.6, 99.9, 99.7 (CH, Ar and

alkene), 55.4 (2 x OCH_3), 51.0, 46.0, 27.5, 26.4 (CH_2). EI-HRMS $(M + H)^+$ found 377.1975, calculated for $C_{22}H_{25}N_4O_2$ 377.1972.

5.1.5 General method for the preparation of amines 16 and 17. To a solution of azide-1*H*-indole (**14** or **15**) (2 mmols) in dry THF (6 mL) was added triphenylphosphine (2.4 mmols) and the reaction stirred at room temperature until evolution of nitrogen ceased (about 1 h). H_2O (0.4 mL, 22 mmols) was added to the reaction mixture which was heated at 60˚C for 2 h. The reaction mixture was concentrated under reduced pressure. The residue was stirred for 20 min with aqueous 2 M HCl (20 mL) and then extracted with CH_2Cl_2 (2 x 20 mL). To the aqueous layer was added aqueous 1 M NaOH (50 mL) until basic pH. The aqueous solution was then extracted with EtOAc (2 x 100 mL), dried ($MgSO_4$) and the solvent removed under reduced pressure to afford the pure product as a glue.

5.1.5.1. 3-(4-Styryl-indol-1-yl)propylamine (16a, R = H). Obtained in 77% yield as a yellow glue. TLC (CH_2Cl_2, R*f* = 0.16). ^{1}H NMR ($CDCl_3$): δ 7.61 (d, *J* = 7.4 Hz, 2H, Ar), 7.55 (d, *J* = 16.3 Hz, 1H, alkene), 7.37-7.43 (m, 3H, Ar), 7.23-7.35 (m, 4H, Ar and alkene), 7.21 (d, *J* = 3.0 Hz, 1H, indole), 6.82 (d, *J* = 3.0 Hz, 1H, indole), 4.27 (t, *J* = 6.8 Hz, 2H, CH_2), 2.75 (t, *J* = 6.9 Hz, 2H, CH_2), 2.02 (m, 2H, CH_2), 1.67 (bs, 2H, -$CH_2N\underline{H_2}$). ^{13}C-NMR ($CDCl_3$): δ 138.0, 136.4, 129.9, 126.9 (C, Ar), 129.3, 128.5, 128.1, 127.3, 127.3, 126.4, 121.7, 117.1, 108.8, 99.7 (CH, Ar and alkene), 43.9, 39.3, 33.7 (CH_2). EI-HRMS $(M + H)^+$ found 277.1701, calculated for $C_{19}H_{21}N_2$ 277.1699.

5.1.5.2. 3-[4-(3,5-Dimethoxystyryl)-indol-1-yl]propylamine (16b, R = OCH_3). Obtained in 72% yield as a yellow glue. TLC (1:1 Petroleum ether/EtOAc R*f* = 0.15). ^{1}H NMR ($CDCl_3$): δ 7.50 (d, *J* = 16.2 Hz, 1H, alkene), 7.36 (d, *J* = 7.2 Hz, 1H, Ar), 7.21-7.29 (m, 3H, Ar, and alkene), 7.16 (d, *J* = 3.2 Hz, 1H, indole), 6.81 (dd, $J_{x,a}$ = 0.8 Hz, $J_{x,b}$ = 2.6 Hz, 1H, indole) 6.74 (d, *J* = 2.3 Hz, 2H, Ar), 6.42 (d, *J* = 2.3 Hz, 1H, Ar), 4.29 (t, *J* = 6.7 Hz, 2H, CH_2), 3.88 (s, 6H, 2 x OCH_3), 3.87 (bs, 2H, -$CH_2N\underline{H_2}$),

3.29 (t, *J* = 6.3 Hz, 2H, CH_2), 2.11 (m, 2H, CH_2). ^{13}C-NMR ($CDCl_3$): δ 161.0 (C), 140.0, 136.3, 129.8, 127.0 (C, Ar), 129.4, 128.1, 127.7, 121.9, 117.4, 108.7, 104.6, 100.2, 99.7 (CH, Ar and alkene), 55.4 (2 x OCH_3), 48.3, 43.2, 29.3 (CH_2). EI-HRMS $(M + H)^+$ found 337.1911, calculated for $C_{21}H_{25}N_2O_2$ 337.1911.

5.1.5.3. 4-(4-Styryl-indol-1-yl)butylamine (17a, R = H). Obtained in 60% yield as a yellow glue. TLC (CH_2Cl_2, R*f* = 0.16). ^{1}H NMR ($CDCl_3$): δ 7.61 (d, *J* = 7.3 Hz, 2H, Ar), 7.44-7.58 (m, 4H, Ar and alkene), 7.26-7.35 (m, 4H, Ar and alkene), 7.19 (d, *J* = 3.1 Hz, 1H, indole), 6.81 (t, *J* = 3.1 Hz, 1H, indole), 4.18 (t, *J* = 6.9 Hz, 2H, CH_2), 2.72 (t, *J* = 7.0 Hz, 2H, CH_2), 1.88-1.94 (m, 4H, CH_2, -$CH_2N\underline{H}_2$), 1.49 (m, 2H, CH_2). ^{13}C-NMR ($CDCl_3$): δ 138.0, 136.4, 129.9, 127.3 (C, Ar), 129.2, 128.7, 128.4, 128.0, 127.0, 126.4, 121.6, 117.1, 108.8, 99.6 (CH, Ar and alkene), 46.4, 41.7, 30.9, 27.2 (CH_2). EI-HRMS $(M + H)^+$ found 291.1857, calculated for $C_{20}H_{23}N_2$ 291.1856.

5.1.5.4. 4-[4-(3,5-Dimethoxystyryl)-indol-1-yl]butylamine (17b, R = OCH_3). Obtained in 79% yield as a yellow glue. TLC (1:1 Petroleum ether/EtOAc R*f* = 0.16). ^{1}H NMR ($CDCl_3$): δ 7.51 (d, *J* = 16.2 Hz, 1H, alkene), 7.38 (d, *J* = 7.1 Hz, 1H, Ar), 7.23-7.30 (m, 3H, Ar and alkene), 7.17 (d, *J* = 3.3 Hz, 1H, indole), 6.76 (d, *J* = 3.1 Hz, 1H, indole), 6.74 (d, *J* = 2.2 Hz, 2H, Ar), 6.42 (d, *J* = 2.3 Hz, 1H, Ar), 4.24 (m, 2H, CH_2), 3.86 (s, 6H, 2 x OCH_3), 3.36 (bs, 4H, CH_2, -$CH_2N\underline{H}_2$), 1.90 (m, 2H, CH_2), 1.70 (m, 2H, CH_2). ^{13}C-NMR ($CDCl_3$): δ 161.0 (C), 133.8, 133.6, 132.0, 131.9 (C, Ar), 129.2, 128.1, 127.7, 121.7, 117.3, 108.9, 104.6, 99.8, 99.7 (CH, Ar and alkene), 55.4 (2 x OCH_3), 45.9, 30.3, 28.9, 23.7 (CH_2). EI-HRMS $(M + H)^+$ found 351.2070, calculated for $C_{22}H_{27}N_2O_2$ 351.2067.

5.1.6 General method for the preparation of benzenesulfonamides 18 and 19. Toluenesulfonyl chloride (1 mmol) and indole amine (**16** or **17**) (1.1 mmol) were

dissolved in dry CH_2Cl_2 (10 mL) under nitrogen atmosphere. The mixture was treated dropwise with triethylamine (2.2 mmol) under ice-cooling and then stirred for 30 min at 0˚C. On completion, the reaction mixture was washed with aqueous 2 M HCl (2 x 30 mL) and with brine (25 mL). Evaporation of the organic solvent after drying over $MgSO_4$ gave the crude compound. The product was isolated by flash column chromatography or recrystallisation giving the desired compound.

5.1.6.1. 4-Methyl-*N*-[3-(4-styryl-indol-1-yl)propyl]benzenesulfonamide (18a, R = H). Obtained in 39% yield as a white solid after recrystallisation from ethyl acetate/hexane. TLC (CH_2Cl_2, R*f* = 0.30). M.p. 130-132 ^oC. ^1H-NMR ($CDCl_3$): δ 7.69 (d, J = 8.2 Hz, 2H, Ar), 7.60 (d, J = 7.4 Hz, 2H, Ar), 7.53 (d, J = 16.3 Hz, 1H, alkene), 7.38-7.42 (m, 3H, Ar), 7.28-7.33 (m, 4H, Ar and alkene), 7.21-7.24 (m, 2H, Ar), 7.15 (d, J = 3.1 Hz, 1H, indole), 6.79 (d, J = 3.1 Hz, 1H, indole), 4.45 (t, J= 6.5 Hz, 1H, -$CH_2N\underline{H}$-SO_2PhCH_3), 4.23 (t, J= 6.5 Hz, 2H, CH_2), 2.92 (q, J= 6.5 Hz, 2H, CH_2), 2.43(s, 1H, CH_3), 2.04 (m, 2H, CH_2). ^{13}C-NMR ($CDCl_3$): δ 143.6, 137.9, 136.4, 136.2, 130.1, 127.6 (C, Ar), 129.8, 129.4, 128.6, 128.1, 127.4, 127.1, 127.0, 126.5, 121.9, 117.2, 108.6, 100.1 (CH, Ar and alkene), 43.3, 40.5, 30.0 (CH_2), 21.5 (CH_3). EI-HRMS $(M + H)^+$ found 431.1783, calculated for $C_{26}H_{27}N_2O_2S$ 431.1788.

5.1.6.2. *N*-(3-{4-[2-(3,5-dimethoxy-phenyl)-vinyl]-indol-1yl}-propyl)-4-methyl-benzenesulfonamide (18b, R = OCH_3). A white solid was obtained in 45% yield after purification by flash column chromatography (dichloromethane). TLC (CH_2Cl_2, R*f* = 0.40). M.p. 142-144 ^oC. ^1H-NMR ($CDCl_3$): δ 7.68 (d, J = 8.3 Hz, 2H, Ar), 7.50 (d, J = 16.4 Hz, 1H, alkene), 7.37 (m, 1H, Ar), 7.28 (d, J = 8.3 Hz, 2H, Ar), 7.24 (d, J = 16.4 Hz, 1H, alkene) 7.22 (d, J = 4.4 Hz, 2H, Ar), 7.10 (d, J = 3.1 Hz, 1H, indole), 6.79 (d, J= 3.3 Hz, 1H, indole), 6.76 (d, J = 2.2 Hz, 2H, Ar), 6.44 (t, J= 2.2 Hz, 1H, Ar), 4.44 (t, J= 6.4 Hz, 1H, -$CH_2N\underline{H}$-SO_2PhCH_3), 4.23 (t, J = 6.6 Hz, 2H, CH_2), 3.88

(s, 6H, 2 x OCH_3), 2.92 (q, J= 6.5 Hz, 2H, CH_2), 2.43 (s, 1H, CH_3), 2.04 (m, 2H, CH_2). ^{13}C-NMR ($CDCl_3$): δ 161.0 (C), 143.6, 139.9, 136.4, 136.2, 129.8, 127.6 (C, Ar), 129.8, 129.4, 128.1, 127.6, 127.0, 121.9, 117.4, 108.7, 104.6, 100.1, 99.8 (CH, Ar and alkene), 55.4 (2 x OCH_3), 43.3, 40.5, 30.0 (CH_2), 2.5 (CH_3). EI-HRMS $(M + H)^+$ found 491.1989, calculated for $C_{28}H_{31}N_2O_4S$ 491.1999.

5.1.6.3. 4-Methyl-*N*-[4-(4-styryl-indol-1-yl)butyl]benzenesulfonamide (19a, R = H). A yellow glue was obtained in 33% yield after purification by flash column chromatography (petroleum ether – ethyl acetate 100:0 v/v increasing to 80:20 v/v). TLC (dichloromethane) R_f 0.40. ^{1}H-NMR ($CDCl_3$): δ 7.71 (d, *J* = 8.2 Hz, 2H, Ar), 7.61 (d, *J* = 7.4 Hz, 2H, Ar), 7.53 (d, *J* = 16.3 Hz, 1H, alkene), 7.36-7.42 (m, 3H, Ar), 7.28-7.33 (m, 4H, Ar and alkene), 7.23 (d, *J* = 4.4 Hz, 2H, Ar), 7.11 (d, *J* = 3.1 Hz, 1H, indole), 6.79 (d, *J* = 3.2 Hz, 1H, indole), 4.43 (t, *J* = 6.3 Hz, 1H, -CH_2N<u>H</u>-SO_2PhCH_3), 4.13 (t, *J* = 6.5 Hz, 2H, CH_2), 2.92 (q, *J* = 6.7 Hz, 2H, CH_2), 2.43 (s, 1H, CH_3), 1.87 (m, 2H, CH_2), 1.47 (m, 2H, CH_2). ^{13}C-NMR ($CDCl_3$): δ 143.5, 137.9, 136.8, 136.3, 129.9, 126.9 (C, Ar), 129.7, 129.3, 128.6, 127.9, 127.4, 127.2, 127.0, 126.4, 121.8, 117.1, 108.7, 99.8 (CH, Ar and alkene), 45.8, 42.6, 27.1, 27.1 (CH_2), 21.5 (CH_3). EI- HRMS $(M + H)^+$ found 445.1944, calculated for $C_{27}H_{29}N_2O_2S$ 445.1944.

5.1.6.4 *N*-(4-{4-[2-(3,5-dimethoxy-phenyl)-vinyl]-indol-1yl}-butyl)-4-methyl-benzenesulfonamide (19b, R = OCH_3). A yellow glue was obtained in 20% yield after purification by flash column chromatography (dichloromethane). TLC (dichloromethane) R_f 0.24. ^{1}H-NMR ($CDCl_3$): δ 7.71 (d, *J* = 8.3 Hz, 2H, alkene), 7.50 (d, *J* = 16.3 Hz, 1H, alkene), 7.36 (m, 1H, Ar), 7.22-7.29 (m, 5H, Ar and alkene), 7.11 (d, *J* = 3.3 Hz, 1H, indole), 6.78 (d, *J* = 3.3 Hz, 1H, indole), 6.76 (d, *J* = 2.1 Hz, 2H, Ar), 6.44 (t, *J* = 2.1 Hz, 1H, Ar), 4.47 (t, *J* = 6.4 Hz, 1H, -CH_2N<u>H</u>-SO_2PhCH_3), 4.12

(t, J = 6.6 Hz, 2H, CH_2), 3.87 (s, 6H, 2 x OCH_3), 2.92 (dd, $J_{x,a}$ = 6.6 Hz, $J_{x,b}$ = 6.8 Hz, 2H, CH_2), 2.42 (s, 1H, CH_3), 1.86 (m, 2H, CH_2), 1.47 (m, 2H, CH_2). ^{13}C-NMR ($CDCl_3$): δ 161.0 (C), 143.4, 140.0, 136.8, 136.3, 129.8, 126.9 (C, Ar), 129.7, 129.4, 128.0, 127.7, 127.0, 121.7, 117.3, 108.8, 104.6, 99.8, 99.7 (CH, Ar and alkene), 55.4 (2 x OCH_3), 45.8, 42.6, 27.1, 27.0 (CH_2), 21.5 (CH_3). EI-HRMS $(M + H)^+$ found 505.2150, calculated for $C_{29}H_{33}N_2O_4S$ 505.2156.

5.1.7 Synthesis of (*E*)-3-(4-styryl-1*H*-indol-1-yl)propyl benzenesulfinate (**20**). To a solution of 1-(3-bromopropyl)-4-styryl-1*H*-indole (**4a**) (2.9 mmol) in DMF (10 mL) was added benzene sulfinic acid sodium salt (2.9 mmol) and the reaction stirred at room temperature for 24 h. The reaction mixture was then evaporated in *vacuo* and the residue was dissolved in CH_2Cl_2 (100 mL), extracted with H_2O (2 x 50 mL) and dried over $MgSO_4$. The organic layer was reduced in *vacuo* and the crude compound was purified by column chromatography (petroleum ether-EtOAc 100:0 v/v increasing to 70:30 v/v) giving a yellow oil in 53% yield. TLC (petroleum ether – EtOAc 7:3 v/v) R_f 0.29. ^{1}H-NMR ($CDCl_3$): δ 7.87 (d, J = 8.2 Hz, 2H, Ar), 7.63 (m, 1H, Ar), 7.60 (d, J = 7.5 Hz, 2H, Ar), 7.51-7.55 (m, 3H, Ar and alkene), 7.38-7.41 (m, 3H, Ar), 7.27-7.32 (m, 2H, Ar and alkene), 7.22 (m, 2H, Ar), 7.15 (d, J = 3.2 Hz, 1H, indole), 6.81 (d, J = 3.2 Hz, 1H, indole), 4.32 (t, J = 6.7 Hz, 2H, CH_2), 3.01 (t, J = 6.9 Hz, 2H, CH_2), 2.32 (m, 2H, CH_2). ^{13}C-NMR ($CDCl_3$): δ 138.9, 137.8, 136.3, 130.1, 129.3, 127.0 (C, Ar), 133.8, 129.5, 128.6, 127.9, 127.7, 127.4, 127.1, 126.5, 122.1,

117.3, 108.6, 100.5 (CH, Ar and alkene), 60.3, 53.0, 44.3 (CH_2). EI-HRMS $(M + H)^+$ found 402.1523, calculated for $C_{25}H_{24}NO_2S$ 402.1522.

5.1.8 General method for the preparation of the ethyl esters (21). The styryl indole derivatives (**3**) (4.3 mmol) and NaH (60% dispersion in mineral oil) (12.9 mmol) in dry DMF (20 mL) were cooled to 0˚C using an ice bath and stirred for 5 min. Ethyl-3-bromopropionate (12.9 mmol) was added and the reaction mixture was stirred for 2 h at room temperature. On completion, the solvent was evaporated under reduced pressure and the residue was dissolved in CH_2Cl_2 (100 mL), washed with H_2O (2 x 50 mL) and dried over $MgSO_4$. The organic layer was then evaporated to dryness.

5.1.8.1 3-(4-Styryl-indol-1-yl)-propionic acid ethyl ester (21a, R = H). A yellow oil was obtained in 60% yield after purification by flash column chromatography (petroleum ether then CH_2Cl_2). TLC (CH_2Cl_2) R_f 0.83. ^{1}H-NMR ($CDCl_3$): δ 7.64 (d, *J* = 7.7 Hz, 2H, Ar), 7.59 (d, *J* = 16.2 Hz, 1H, alkene), 7.42-7.45 (m, 3H, Ar), 7.29-7.37 (m, 4H, Ar and alkene), 7.26 (d, *J* = 3.2 Hz, 1H, indole), 6.85 (d, *J* = 3.2 Hz, 1H, indole), 4.59 (t, *J* = 6.9 Hz, 2H, CH_2), 4.18 (q, *J* = 7.2 Hz, 2H, CH_2), 3.34 (t, *J* = 6.1 Hz, 2H, CH_2), 2.87 (t, *J* = 6.9 Hz, 2H, CH_2), 1.26 (t, *J* = 7.2 Hz, 3H, CH_3). ^{13}C-NMR ($CDCl_3$): δ 171.1 (C), 137.9, 136.1, 130.0, 127.1 (C, Ar), 129.4, 128.6, 128.2, 127.4, 127.1, 126.5, 121.9, 117.5, 117.3, 108.5, 101.3, 100.2 (CH, Ar and alkene),

60.9, 42.0, 35.0 (CH_2), 14.1 (CH_3). EI-HRMS $(M + H)^+$ found 320.1648, calculated for $C_{21}H_{22}NO_2$ 320.1645.

5.1.8.2 3-{4-[2-(3,5-Dimethoxy-phenyl)-vinyl]-indol-1-yl}-propionic acid ethyl ester (21b, R = OCH_3). A yellow oil was obtained in 53% yield after purification by flash column chromatography (petroleum ether then CH_2Cl_2). TLC (CH_2Cl_2) R_f 0.71. ^{1}H-NMR ($CDCl_3$): δ 7.52 (d, *J* = 16.3 Hz, 1H, alkene), 7.39 (d, *J* = 7.2 Hz, 1H, Ar), 7.30-7.36 (m, 2H, Ar and alkene), 7.27 (d, *J* = 7.2 Hz, 1H, Ar), 7.24 (d, *J* = 3.2 Hz, 1H, indole), 6.81 (d, *J* = 3.1 Hz, 1H, indole), 6.78 (d, *J* = 2.0 Hz, 2H, Ar), 6.45 (t, *J* = 2.0 Hz, 1H, Ar), 4.50 (t, *J* = 6.9 Hz, 2H, CH_2), 4.15 (q, *J* = 7.2 Hz, 2H, CH_2) , 3.88 (s, 6H, 2 x OCH_3), 2.86 (t, *J* = 6.9 Hz, 2H, CH_2), 1.24 (t, *J* = 7.2 Hz, 3H, CH_3). ^{13}C-NMR ($CDCl_3$): δ 171.1 (C), 161.0 (C), 140.0, 136.1, 129.8, 127.1 (C, Ar), 129.3, 128.3, 127.7, 121.9, 117.4, 108.7, 104.6, 100.1, 99.7 (CH, Ar and alkene), 55.4 (2 x OCH_3), 60.9, 42.0, 35.0 (CH_2), 14.1 (CH_3). EI-HRMS $(M + H)^+$ found 380.1859, calculated for $C_{23}H_{26}NO_4$ 380.1856.

5.1.9 General method for the preparation of 3- styryl indole propanol derivatives (**22**). A solution of *3*-ethyl styryl indole propionate derivative (**21**) (2.1 mmol) in dry THF (12 mL) under nitrogen atmosphere was cooled to 0˚C. $LiAlH_4$ (1M solution in THF) (8.4 mmol) was added dropwise via syringe. The yellow reaction mixture was

stirred at 0˚C for 1 h, then at room temperature for 4 h. The reaction was quenched by the addition of EtOAc (70 mL), the organic layer was washed with H_2O (3 x 50 mL), dried over $MgSO_4$, and evaporated to dryness.

5.1.9.1 3-(4-Styryl-indol-1-yl)-propan-1-ol (22a, R = H). A yellow-orange wax was obtained in 20% after purification by flash column chromatography (CH_2Cl_2). TLC (CH_2Cl_2) R_f 0.28. ^{1}H-NMR ($CDCl_3$): δ 7.61 (d, *J* = 7.3 Hz, 2H, Ar), 7.56 (d, *J* = 16.5 Hz, 1H, alkene), 7.39-7.42 (m, 3H, Ar), 7.35 (d, *J* = 7.4 Hz, 2H, Ar), 7.24-7.31 (m, 3H, Ar and alkene), 7.23 (d, *J* = 3.2 Hz, 1H, indole), 6.83 (d, *J* = 3.2 Hz, 1H, indole), 4.33 (t, *J* = 6.8 Hz, 2H, CH_2) , 3.64 (t, *J* = 5.8 Hz, 2H, CH_2), 2.10 (m, 2H, CH_2), 1.37 (bs, 1H, -CH_2O<u>H</u>). ^{13}C-NMR ($CDCl_3$): δ 138.0, 136.5, 129.9, 127.0 (C, Ar), 129.3, 128.6, 128.2, 127.3, 127.2, 126.4, 121.7, 117.1, 108.8, 99.8 (CH, Ar and alkene), 59.5, 42.8, 32.6 (CH_2). EI-HRMS $(M + H)^+$ found 278.1539, calculated for $C_{19}H_{20}NO$ 278.1539.

5.1.9.2 3-{4-[2-(3,5-Dimethoxy-phenyl)-vinyl]-indol-1-yl}-propan-1-ol (22b, R = OCH_3). A brownish wax was obtained in 48% yield after purification by flash column chromatography (CH_2Cl_2-MeOH 100:0 v/v increasing to 98:2 v/v). TLC (CH_2Cl_2) R_f 0.20. ^{1}H-NMR ($CDCl_3$): δ 7.52 (d, *J* = 16.4 Hz, 1H, alkene), 7.34-7.38 (m, 2H, Ar), 7.22-7.27 (m, 3H, Ar, alkene and indole), 6.81 (d, *J* = 3.1 Hz, 1H, indole), 6.77 (d, *J* = 2.1 Hz, 2H, Ar), 6.44 (t, *J* = 2.1 Hz, 1H, Ar), 4.33 (t, *J* = 6.7 Hz, 2H, CH_2), 3.88 (s, 6H, 2 x OCH_3), 3.63 (t, *J* = 5.9 Hz, 2H, CH_2), 2.10 (m, 2H, CH_2),

1.65 (bs, 1H, -$CH_2O\underline{H}$). ^{13}C-NMR ($CDCl_3$): δ 161.0 (C), 140.0, 136.5, 129.7, 126.9 (C, Ar), 129.2, 128.3, 127.7, 121.7, 117.3, 108.9, 104.6, 99.7, 99.6 (CH, Ar and alkene), 55.4 (2 x OCH_3), 59.4, 42.8, 35.6 (CH_2). EI-HRMS $(M + H)^+$ found 338.1755, calculated for $C_{21}H_{24}NO_3$ 338.1751.

5.1.10 General method for the synthesis of toluene-sulfonic acid 3-styryl indole propyl ester derivatives (23). To a cooled (0˚C) solution of 3-styryl indole propanol derivative (**22**) (0.9 mmol) and 4-dimethylaminopyridine (0.2 mmol) in dry CH_2Cl_2 (7 mL) and pyridine (0.7 mL) under nitrogen atmosphere was added 4-toluenesulfonyl chloride (2 mmol) portion-wise. The reaction was stirred at 0˚C for 10 min then stirred for 24 h at room temperature. On the completion, the reaction mixture was washed with aqueous satured $NaHCO_3$ (50 mL) and the organic layer was separated. The aqueous layer was extracted with CH_2Cl_2 (50 mL) and both organic layers were washed with aqueous 1 M HCl (50 mL). The organic layer was washed with aqueous saturated $NaHCO_3$ (50 mL) and then dried over $MgSO_4$. The solvent was evaporated under vacuum.

5.1.10.1 Toluene-4-sulfonic acid 3-(4-styryl-indol-1-yl)-propyl ester (23a, R = H). A yellow glue was obtained in 53% yield after purification by flash column chromatography (petroleum ether – ethyl acetate 100:0 v/v increasing to 90:10 v/v). TLC (petroleum ether – ethyl acetate 8:2 v/v) R_f 0.48. ^{1}H-NMR ($CDCl_3$): δ 7.78 (d, *J*

= 8.2 Hz, 2H, Ar), 7.60 (d, *J* = 7.1 Hz, 2H, Ar), 7.52 (d, *J* = 16.4 Hz, 1H, alkene), 7.29-7.42 (m, 7H, Ar and alkene), 7.20-7.24 (m, 3H, Ar), 7.04 (d, *J* = 3.2 Hz, 1H, indole), 6.74 (d, *J* = 3.2 Hz, 1H, indole), 4.26 (t, *J* = 6.5 Hz, 2H, CH_2) , 3.99 (t, *J* = 5.5 Hz, 2H, CH_2), 2.47 (s, 3H, CH_3), 2.20 (m, 2H, CH_2). ^{13}C-NMR ($CDCl_3$): δ 145.0, 139.9, 136.1, 132.7, 130.0, 127.0 (C, Ar), 129.9, 129.4, 128.6, 128.1, 127.9, 127.4, 127.1, 126.4, 121.9, 117.2, 108.5, 100.1 (CH, Ar and alkene), 67.0, 42.2, 29.4 (CH_2), 21.6 (CH_3). EI-HRMS $(M + H)^+$ found 432.1627, calculated for $C_{26}H_{26}NO_3S$ 432.1628.

5.1.10.2 Toluene-4-sulfonic acid 3-{4-[2-(3,5-dimethoxy-phenyl)-vinyl]-indol-1-yl}-propyl ester (23b, R = OCH_3). A yellow-orange glue was obtained in 50% yield after purification by flash column chromatography (petroleum ether – ethyl acetate 100:0 v/v increasing to 80:20 v/v). TLC (petroleum ether – ethyl acetate 1:1 v/v) R_f 0.57. ^{1}H-NMR ($CDCl_3$): δ 7.78 (d, *J* = 8.2 Hz, 2H, Ar), 7.48 (d, *J* = 16.5 Hz, 1H, alkene), 7.33-7.37 (m, 3H, Ar), 7.21-7.24 (m, 3H, Ar and alkene), 7.04 (d, *J* = 3.1 Hz, 1H, indole), 6.76 (d, *J* = 2.2 Hz, 2H, Ar), 6.74 (d, *J* = 3.1 Hz, 1H, indole), 6.44 (t, *J* = 2.2 Hz, 1H, Ar), 4.26 (t, *J* = 6.6 Hz, 2H, CH_2), 3.99 (t, *J* = 5.7 Hz, 2H, CH_2), 3.88 (s, 6H, 2 x OCH_3), 2.47 (s, 3H, CH_3), 2.04 (m, 2H, CH_2). ^{13}C-NMR ($CDCl_3$): δ 161.0 (C), 145.0, 139.9, 136.1, 132.7, 129.8, 127.6 (C, Ar), 129.9, 129.4, 128.1, 27.9, 127.1, 121.9, 117.4, 108.6, 104.6, 100.1, 99.7 (CH, Ar and alkene), 55.4 (2 x OCH_3), 67.0, 42.2, 29.4 (CH_2), 21.6 (CH_3). EI-HRMS $(M + H)^+$ found 492.1831, calculated for

$C_{28}H_{30}NO_5S$ 492.1839.

5.2 CYP24A1 and CYP27B1 inhibition assay

Inhibition of CYP24A1 was carried out as described previously [23]. Briefly, reaction mixture containing 0.1 μM each of Adx and AdR, 0.075 μM MBP-CYP24A1, 2.5 μM 1,25$(OH)_2D_3$, varying concentrations of inhibitors, and 0.5 mM NADPH was incubated at 37 °C for 25 min in a buffer of 20 mM Tris (pH 7.5) and 125 mM NaCl. All inhibitors were dissolved in ethanol (>10 mM) or DMSO (>50 mM) and further diluted in ethanol to make working stock (<1 mM). The reaction was extracted with CH_2Cl_2 and analyzed by HPLC. The IC_{50} values were determined by fitting the relative activity (V/V_0) against the inhibitor concentration [I] using the equation $V/V_0 = IC_{50}/(IC_{50} + [I])$, where V and V_0 are the reaction rates in the presence and absence of inhibitors. The assay for each compound was performed in at least duplicate and in triplicate for compounds with good inhibitory properties.

The K_I values were calculated using equation $K_I = IC_{50}/(1 + [S]/K_M)$, where [S] is the substrate concentration and K_M = 0.19 μM [14].

Inhibition assay of CYP27B1 was performed in a similar way to that of CYP24A1 as previously described [23]. The concentration of substrate 25$(OH)D_3$ was 2.5 μM and K_M for CYP27B1 was 0.48 μM.

5.3 Molecular Modelling

Docking studies were performed using LeadIT2.1.2 docking program by BioSolve.IT [29]. The important amino acid residues of the active pocket (Gln82, Ile131, Trp134, Met246, Ala326, Glu329, Thr330, Val391, Phe393, Thr394, Ser498, Gly499, Tyr500) [32] were selected and then the selection was extended to 12 Å in order to include in

the docking site the haem iron region and the access tunnel to the catalytic site. A ligands database in mol2 format, prepared using MOE [30], was used as input for the docking calculations. The iron atom of the catalytic site was set as essential pharmacophoric feature. Ligand docking was performed using the default values and no water molecules were considered. Ten output solutions were obtained from each compound and visual inspection in MOE was used to identify the interaction between ligand and protein.

The flexible alignment studies were performed using MOE 2010. The MOE flexible alignment tool generates different possible conformations for each of the different six molecules present in the input mol2 format database that could overlap with the assigned template. The quality of the alignment is evaluated by a score which is a sum of the internal strain of the obtained conformation (the smaller, the better) and the overlap of molecular features (aromatic regions, donors/acceptors). MOE, for each alignment performed, evaluates the average internal energy of the ligands U, the similarity score F (the lower value is the better two structures overlap) and the value S (sum of U and F values obtained for each alignment). A good alignment should present a dU value (the average strain energy of the molecules in the alignment in kcal/mol) lower than 1 kcal/mol meaning that the obtained conformation are not energetically disadvantaged. In our case, we kept our template rigid and the flexible alignment of the six compounds was run. The obtained data with a dU of 0.0 (no energy penalty) were kept and ranked according to the lowest S value.

Acknowledgements

We acknowledge Cancer Research UK for funding (SF, Grant Ref. C7735/

A10649), the Embassy of the Arab Republic of Egypt (MSG, PhD scholarship) and the EPSRC Mass Spectrometry Centre, Swansea, UK for mass spectroscopy data.

References

[1] K.K. Deeb, D.L. Trump, C.S. Johnson. Vitamin D signalling pathways in cancer: potential for anticancer therapeutics. Nat. Rev. Cancer 7 (2007) 684–700.

[2] H.A.Morris. Vitamin D: a hormone for all seasons—how much is enough? Clin. Biochem. Rev. 26 (2005) 21–32.

[3] H.F. DeLuca. Overview of general physiologic features and functions of vitamin D. Am. J. Clin. Nutr. 80 (2004) 1689S-1696S.

[4] T.E. Robsahm, S. Tretli, A. Dahlback, J. Moan. Vitamin D3 from sunlight may improve the prognosis of breast-, colon- and prostate cancer (Norway). Cancer Causes Control 15 (2004) 149–158.

[5] W. Zhou, R.S. Heist, G. Liu, K. Asomaning, D.S. Neuberg, B.W. Hollis, J.C. Wain, T.J. Lynch, E. Giovannucci, L. Su, D.C. Christiani. Circulating 25-hydroxyvitamin D levels predict survival in early- stage non-small-cell lung cancer patients. J. Clin. Oncol. 25 (2007) 479–485.

[6] S. Swaimi, A.V. Krishnan, D. Feldman. Vitamin D metabolism and action in the prostate: implications for health and disease. Mol. Cell. Endocrinol. 347 (2011) 61-69.

[7] L. Lipworth, M. Rossi, J.K. McLaughlin, E. Negri, R. Talamini, F. Levi, S. Franceschi, C. La Vecchia. Dietary vitamin D and cancers of the oral cavity and esophagus. Ann. Oncol. 20 (2009) 1576–1581.

[8] J. Wactawski-Wende, J.M. Kotchen, G.L. Anderson, A.R. Assaf, R.L. Brunner, M.J. O'Sullivan, K.L. Margol, J.K. Ockene, L. Phillips, L. Pottern, R.L. Prentice, J.

Robbins, T.E. Rohan, G.E. Sarto, S. Sharma, M.L. Stefanick, L. Van Horn, R.B. Wallace, E. Whitlock, T. Bassford, S.A.A. Beresford, H.R. Black, D.E. Bonds, R.G. Brzyski, B. Caan, R.T. Chlebowski, B. Cochrane, C. Garland, M. Gass, J. Hays, G. Heiss, S.L. Hendrix, B.V. Howard, J. Hsia, F.A. Hubbell, R.D. Jackson, K.C. Johnson, H. Judd, C.L. Kooperberg, L.H. Kuller, A.Z. LaCroix, D.S. Lane, R.D. Langer, N.L. Lasser, C.E. Lewis, M.C. Limacher, J.E. Manson. Calcium plus vitamin D supplementation and the risk of colorectal cancer. N. Engl. J. Med. 354 (2006) 684–696.

[9] M. Rossi, J.K. McLaughlin, P. Lagiou, C. Bosetti, R. Talamini, L. Lipworth, A. Giacosa, M. Montella, S. Franceschi, E. Negri, C. La Vecchia. Vitamin D intake and breast cancer risk: a case-control study in Italy. Ann. Oncol. 20 (2009) 374–378.

[10] H. Orell-Kotikangas, U. Schwab, P. Osterlund, K. Saarilahti, O. Makitie, A.A. Makitie. High prevalence of vitamin D insufficiency in patients with head and neck cancer at diagnosis. Head Neck 34 (2012) 1450–1455.

[11] J.A. Omdahl, E.V. Bobrovnikova, A. Annalora, P. Chen, R. Serda, R. Expression, structure-function, and molecular modeling of vitamin D P450s. J. Cell. Biochem. 88 (2003) 356-362.

[12] G. Jones, D.E. Prosser, M. Kaufman, M. 25-Hydroxy vitamin D-24-hydroxylase (CYP24A1): its important role in the degradation of vitamin D. Arch. Biochem. Biophys. 523 (2012) 9-18.

[13] M.G. Anderson, M. Nakane, X. Ruan, P.E. Kroeger, J.R. Wu-Wong. Expression of VDR and CYP24A1 mRNA in human tumors. Cancer Chemother. Pharmacol. 57 (2006) 234–240.

[14] K. Mimori, Y. Tanaka, K. Yoshinaga, T. Masuda, K. Yamashita, M. Okamoto, H. Inoue, M. Mori, M. Clinical significance of the overexpression of the candidate

oncogene CYP24 in esophageal cancer. Ann. Oncol. 15 (2004) 236–241.

[15] H.C. Horvath, P. Lakatos, J.P. Kosa, K. Bacsi, K. Borka, G. Bises, T. Nittke, P.A. Hershberger, G. Speer, E. Kallay, E. The candidate oncogene CYP24A1: a potential biomarker for colorectal tumorigenesis. J. Histochem. Cytochem. 58 (2010) 277–285.

[16] G. Chen, S.H. Kim, A.N. King, L. Zhao, R.U. Simpson, P.J. Christensen, Z.W. Wang, D.G. Thomas, T.J. Giordano, L. Lin, D.E. Brenner, D.G. Beer, N. Ramnath CYP24A1 is an independent prognostic marker of survival in patients with lung adenocarcinoma. Clin. Cancer Res. 17 (2011) 817–826.

[17] J. Zhao, B.K. Tan, S. Marcelis, A. Verstuyf, R. Bouillon. Enhancement of antiproliferative activity of 1α, 25-dihydroxyvitamin D-3 (analogs) by cytochrome P450 enzyme inhibitors is compound- and cell-type specific. J.Steroid Biochem. Mol. Biol. 57 (1996) 197-202.

[18] J.R. Muindi, W.D. Yu, Y. Ma, K.L. Engler, R.X. Kong, D.L. Trump, C.S. Johnson. CYP24A1 inhibition enhances the antitumor activity of calcitriol. Endocrinol. 151 (2010) 4301–4312.

[19] A.V. Krishnan, S. Swami, J. Moreno, R.B. Bhattacharyya, D.M. Peehl, D. Feldman. Potentiation of the growth-inhibitory effects of vitamin D in prostate cancer by genistein. Nutr. Rev. 65 (2007) S121-S123.

[20] S.W. Yee, M.J. Campbell, C. Simons. Inhibition of Vitamin D3 metabolism enhances VDR signalling in androgen-independent prostate cancer cells. J. Steroid Biochem. Mol. Biol. 98 (2006) 228–235.

[21] A.S. Aboraia, S.W. Yee, M.S. Gomaa, N. Shah, A.C. Robotham, B. Makowski, D. Prosser, A. Brancale, G. Jones, C. Simons. Synthesis and CYP24A1 inhibitory

activity of *N*-(2-(1*H*-imidazol-1-yl)-2-phenylethyl)arylamides. Bioorg. Med. Chem. 18 (2010) 4939-4946.

[22] A.S. Aboraia, B. Makowski, A. Bahja, D. Prosser, A. Brancalea, G. Jones, C. Simons. Synthesis and CYP24A1 inhibitory activity of (*E*)-2-(2-substituted benzylidene)- and 2-(2-substituted benzyl)-6-methoxy-tetralones. Eur. J. Med. Chem., 45 (2010) 4427-4434.

[23] J. Zhu, R. Barycki, G. Chiellini, H.F. DeLuca, H.F. Screening of selective inhibitors of 1α,25-dihydroxyvitamin D_3 24-hydroxylase using recombinant human enzyme expressed in *Escherichia coli*. Biochem. 49 (2010) 10403-10411.

[24] B.A. Patel, C.B. Ziegler, N.A. Cortese, J.E. Plevyak, T.C. Zebovitz, M. Terpko, R.F. Heck. Palladium-catalyzed vinylic substitution reactions with carboxylic acid derivatives. J. Org. Chem. 42 (1977) 3903-3907.

[25] F.L. Lin, H.M. Hoyt, H. van Halbeek, R.G. Bergman, C.R. Bertozzi. Mechanistic investigation of the Staudinger ligation. J. Am. Chem. Soc. 127 (2005) 2686-2695.

[26] L. Munoz, E. Rosa, M.P. Bosch, A. Guerrero, A. A new practical and efficient sulfone-mediated synthesis of trifluoromethyl ketones from alkyl and alkenyl bromides. Tetrahedron Lett. 46 (2005) 3311-3313.

[27] C. Billaud, J.P. Goddard, T.L. Gall, C. Mioskowski. Preparation of alcohols from sulfones and trialkylboranes. Tetrahedron Lett. 44 (2003) 4451-4454.

[28] S. Ferla, A. Brancale, H.F. DeLuca, J. Zhu, C. Simons. Small moleculae inhibitors of CYP24A1for treatment of various cancer. Abs. Paper Am. Chem. Soc. 245 (2013) 73-MEDI.

[29] http://www.biosolveit.de/

[30] http://www.chemcomp.com/MOE-Molecular_Operating_Environment.htm

[31] A.J. Annalora, D.B. Goodin, W.H. Hong, Q. Zhang, E.F. Johnson, C.D. Stout.

Crystal structure of CYP24A1, a mitochondrial cytochrome P450 involved in vitamin D metabolism. J. Mol. Biol. 396 (2010) 441-451.

[32] M.S. Gomaa, A. Brancale, C. Simons. Homology model of 1α,25-dihydroxyvitamin D_3 24-hydroxylase cytochrome P450 24A1 9CYP24A1): active site architecture and ligand binding. J. Steroid Biochem. Mol. Biol. 104 (2007) 53-60.

[33] P. Labute, C. Williams. Flexible alignment of small molecules. J. Med. Chem. 44 (2001) 1483-1490.

[34] I. Schuster, H. Egger, P. Nussbaumer, R.T. Kroemer. Inhibitors of vitamin D hydroxylase: structure-activity relationship. J. Cell. Biochem. 88 (2003) 372-380.

[35] I. Schuster, H. Egger, D. Bikle, G. Herzig, G.S. Reddy, A. Stuetz, G. Stuetz, G. Vorisek. Selective inhibitors of vitamin D hydroxylase in human keratinocytes. Steroids. 66 (2001) 409-422.